

Hydrodynamic Fluid Film Bearings and Their Effect on the Stability of Rotating Machinery

Luis San Andrés

Mast-Childs Tribology Professor
Turbomachinery Laboratory, Texas A&M University
College Station, TX 77843-3123
USA

Lsanandres@mengr.tamu.edu

ABSTRACT

The lecture introduces the basic principles of hydrodynamic lubrication and the fundamental equation of Classical Lubrication Theory. The analysis proceeds to derive the static and dynamic performance characteristics of short length cylindrical journal bearings, with application to the dynamic forced performance of a rigid rotor supported on plain bearings. In a radial bearing, the Sommerfeld number defines a relationship between the static load and the journal eccentricity within the bearing. This design parameter shows the static performance of the bearing as rotor speed increases. Rotordynamic force coefficients are introduced and their effect on the stability of a rotor-bearing system thoroughly discussed. Cross-coupled force coefficients are solely due to journal rotation, and the magnitude (and sign) of the cross-stiffness determines rotordynamic stability. The whirl frequency ratio (WFR) relates the whirl frequency of subsynchronous motion to a threshold speed of instability. The desired WFR is null; however, plain cylindrical bearings show a whirl ratio of just 0.50, limiting the operation of rotating machinery to shaft speeds below twice the system first critical speed. The analysis concludes with a review of practical (in use) journal bearing configurations with highlights on their major advantages and disadvantages, including remedies to reduce or entirely avoid subsynchronous whirl instability problems.

1.0 FUNDAMENTS OF FLUID FILM BEARING ANALYSIS

Figure 1 depicts an idealized geometry of a fluid film bearing. The major characteristic of a lubricant film, and which allows a major simplification of its analysis, is that the thickness of the film (h) is very small when compared to its length (L) or to its radius of curvature (R), i.e. (h/L) or $(h/R) \ll \ll 1$.

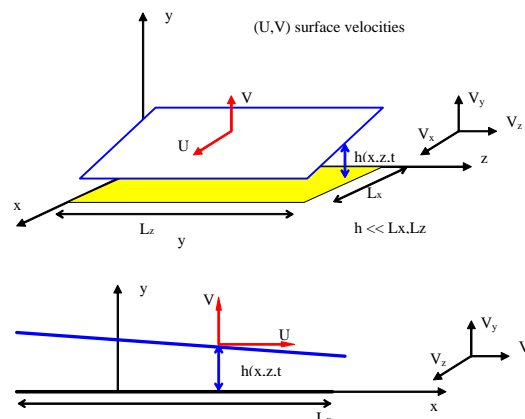


Figure 1: Geometry of Flow Region in a Thin Fluid Film Bearing ($h \ll L_x, L_z$).

San Andrés, L. (2006) Hydrodynamic Fluid Film Bearings and Their Effect on the Stability of Rotating Machinery. In *Design and Analysis of High Speed Pumps* (pp. 10-1 – 10-36). Educational Notes RTO-EN-AVT-143, Paper 10. Neuilly-sur-Seine, France: RTO. Available from: <http://www.rto.nato.int/abstracts.asp>.

Report Documentation Page

*Form Approved
OMB No. 0704-0188*

Public reporting burden for the collection of information is estimated to average 1 hour per response, including the time for reviewing instructions, searching existing data sources, gathering and maintaining the data needed, and completing and reviewing the collection of information. Send comments regarding this burden estimate or any other aspect of this collection of information, including suggestions for reducing this burden, to Washington Headquarters Services, Directorate for Information Operations and Reports, 1215 Jefferson Davis Highway, Suite 1204, Arlington VA 22202-4302. Respondents should be aware that notwithstanding any other provision of law, no person shall be subject to a penalty for failing to comply with a collection of information if it does not display a currently valid OMB control number.

1. REPORT DATE 01 NOV 2006	2. REPORT TYPE N/A	3. DATES COVERED -			
4. TITLE AND SUBTITLE Hydrodynamic Fluid Film Bearings and Their Effect on the Stability of Rotating Machinery		5a. CONTRACT NUMBER			
		5b. GRANT NUMBER			
		5c. PROGRAM ELEMENT NUMBER			
6. AUTHOR(S)		5d. PROJECT NUMBER			
		5e. TASK NUMBER			
		5f. WORK UNIT NUMBER			
7. PERFORMING ORGANIZATION NAME(S) AND ADDRESS(ES) Mast-Childs Tribology Professor Turbomachinery Laboratory Texas A&M University College Station, TX 77843-3123 USA		8. PERFORMING ORGANIZATION REPORT NUMBER			
9. SPONSORING/MONITORING AGENCY NAME(S) AND ADDRESS(ES)		10. SPONSOR/MONITOR'S ACRONYM(S)			
		11. SPONSOR/MONITOR'S REPORT NUMBER(S)			
12. DISTRIBUTION/AVAILABILITY STATEMENT Approved for public release, distribution unlimited					
13. SUPPLEMENTARY NOTES See also ADM002051., The original document contains color images.					
14. ABSTRACT					
15. SUBJECT TERMS					
16. SECURITY CLASSIFICATION OF:			17. LIMITATION OF ABSTRACT UU	18. NUMBER OF PAGES 36	19a. NAME OF RESPONSIBLE PERSON
a. REPORT unclassified	b. ABSTRACT unclassified	c. THIS PAGE unclassified			

A **plain** cylindrical journal bearing, see Figure 2, comprises of an inner rotating cylinder (journal) of radius R_J and an outer cylinder (bearing) of radius $R_B (>R_J)$. The two cylinders are closely spaced and the annular gap between the two cylinders is filled with some lubricant. The radial clearance $c = (R_B - R_J)$ is very small. In most fluid film bearings with incompressible liquids, $c/R_B = 0.001$; while for gas film bearings, $C/R_B = 0.0001$, typically.

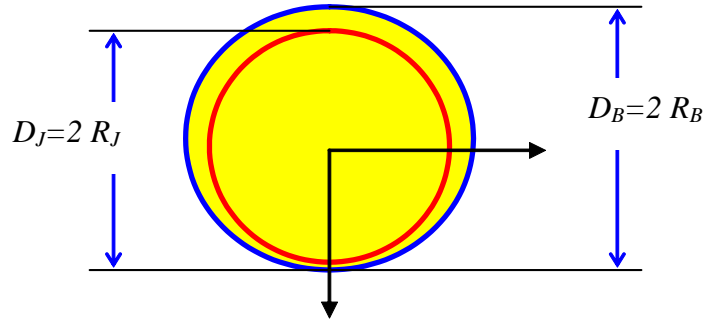


Figure 2: Schematic View of a Cylindrical Bearing.

As a consequence of the smallness in film thickness, **the effects of the film curvature are negligible in the operation of a journal bearing.**

The analysis of the flow equation defines the circumferential flow Reynolds number (Re) as

$$Re = \frac{\rho U_* c}{\mu} \quad \& \quad Re_* = Re (c/L_*) \quad (1a)$$

based on the characteristic speed ($U_* = \Omega R$). Re denotes the ratio between fluid inertia (advection) forces and viscous-shear forces. And,

$$Re_s = \frac{\rho \omega c^2}{\mu} \quad (1b)$$

is the squeeze film Reynolds number representing the ratio between temporal fluid inertia forces due to transient motions at a characteristics frequency (ω) and viscous-shear forces. Fluid inertia effects in thin film flows are of importance only in those applications where both Reynolds numbers are larger than ONE¹, i.e. $Re_*, Re_s \gg 1$.

The film thickness to characteristic length ratio (c/L_*) in thin film flows is typically very small. Thus, fluid inertia terms are to be retained for flows with Reynolds numbers of the order [2]:

$$Re > (L_*/c) \times 1 > 1,000 \quad \text{for } (c/L_*) = 0.001 \quad (2)$$

Classical lubrication is based on the assumption that fluid inertia effects are negligible, i.e. $(Re_s, Re_*) \rightarrow 0$, in most practical applications; and hence, rendering effectively an inertialess fluid.

¹ In actuality, $Re > 12$ for steady super laminar flow in thin film bearings, as demonstrated in [1]. In thin film flows, transition to turbulence is due to instability of shear driven parallel flow. A transition to turbulence initiated by the appearance of Taylor vortices generated by centrifugal forces is more peculiar to configurations with large clearances, i.e. not common in thin film bearings. The accepted Reynolds number for flow turbulence in journal bearings is $Re_c = \rho \Omega R c / \mu > 2,000$ [2].

The thin film laminar flow of an incompressible, inertialess and isoviscous fluid is governed by the following equations continuity and momentum transport equations:

$$\frac{\partial(v_x)}{\partial x} + \frac{\partial(v_y)}{\partial y} + \frac{\partial(v_z)}{\partial z} = 0 \quad ; \quad 0 = -\frac{\partial P}{\partial x} + \mu \frac{\partial^2 v_x}{\partial y^2}; \quad 0 = -\frac{\partial P}{\partial z} + \mu \frac{\partial^2 v_x}{\partial y^2} \quad (3)$$

where $v_{x,y,z}$ are the velocity components and the film pressure (P) is uniform across the film thickness (h). The momentum equations establish a quasi-static balance of pressure and viscous forces. The lubrication equations denote “slow” flow conditions with time appearing as a parameter, not an independent variable.

Table 1 presents the circumferential flow Reynolds numbers (Re) for a typical journal bearing application operating with different fluids. The example bearing is a 3 inch (76 mm) diameter ($2R_j$) journal and the clearance to radius ratio (c/R_j) is 0.001, a typical value for journal bearings. Two rotational speeds of 1,000 and 10,000 rpm ($\Omega=104.7$ and 1047 rad/s) are noted in the table. The calculated Reynolds numbers (**Re**) show that bearing applications with mineral oils and (even) air do not need to include fluid inertia effects, i.e. $Re < 1,000$. However, process fluid applications using water, R134a refrigerant and cryogenic fluids show large Reynolds numbers at a speed of 10,000 rpm.

Table 1: Importance of Fluid Inertia Effects on Several Fluid Film Bearing Applications ($c/R_j=0.001$, $R_j=38.1$ mm (1.5 inch))

Fluid	Absolute viscosity (μ) lbm.ft.s x 10^{-5}	Kinematic viscosity (ν) centistoke	Re at 1,000 rpm	Re at 10,000 rpm
Air	1.23	15.4	9.9	99
Thick oil	1,682	30.0	5.1	51
Light oil	120	2.14	71	711
Water	64	1.00	159	1,588
Liquid hydrogen	1.075	0.216	705	7,052
Liquid oxygen	10.47	0.191	794	7,942
Liquid nitrogen	13.93	0.179	848	8,477
R134 refrigerant	13.30	0.163	930	9,296

Note that current bearing applications using process liquids to replace mineral oils may operate at speeds well above 10,000 rpm. Incidentally, the operating speed of cryogenic turbopumps is on the order of 30 – 70 krpm, and future applications (currently in the works) will operate at speeds close to 200 krpm!

Incidentally, process gas and liquid seals, isolating regions of high and low pressures in a typical compressor or pump, have larger radial clearances than load support fluid film bearings. For example, in water neck-ring and interstage seals in pumps, $R/C \sim 250$, and thus fluid inertia effects are of importance even at relatively low rotational speeds ($\sim 1,000$ rpm and larger). The topic of seals is analyzed in the next lecture.

1.1 Other Fluid Inertia Effects

Fluid inertia within thin film flow domains can be safely ignored in most conventional (oil lubricated) bearing applications. However, fluid inertia effects may also be of great importance at the inlet to the film and discharge from the film sections in a typical pad bearing or seal application, see Figure 3. Depending on the flow conditions upstream of a sudden contraction or a sudden enlargement, a fraction of the dynamic pressure head, typically given as ($\frac{1}{2} \rho U^2$), is lost or recovered.

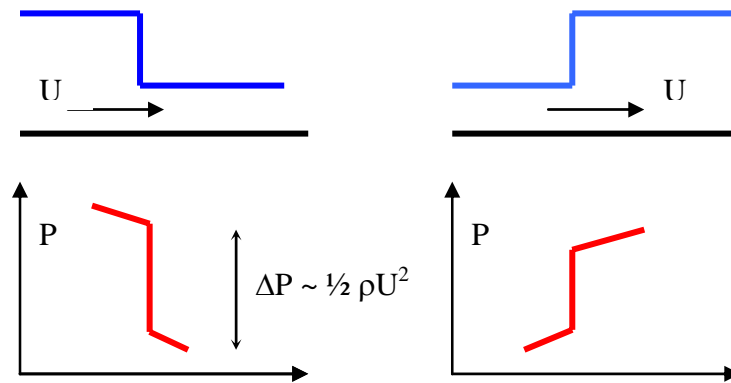
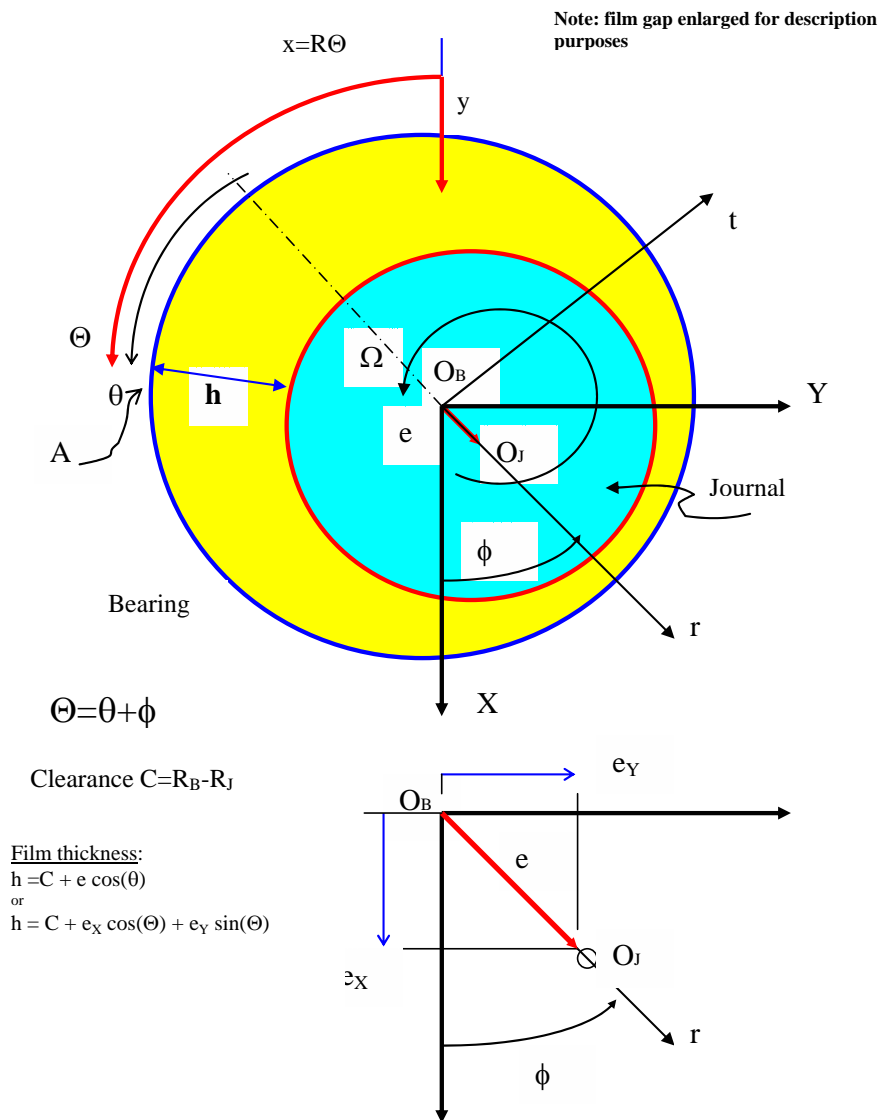


Figure 3: Pressure Drop & Rise at Sudden Changes in Film Thickness.

Sudden pressure losses are typical at the edges of a pocket in a hydrostatic bearing and at the inlet plane of annular pressure seals. The same phenomenon also occurs at the leading edge of a bearing pad in high speed tilting pad bearings. A sudden pressure recovery is also quite typical at the discharge section of a pressurized annular or labyrinth seal. Note that the importance of fluid inertia effects may be restricted only to the inlet and discharge sections, and may not be relevant within the thin film flow domain.

2.0 REYNOLDS EQUATION AND KINEMATICS OF JOURNAL MOTION

Lubricated cylindrical bearings are low friction, load bearing supports in rotating machinery. These fluid film bearings also introduce viscous damping that aids in reducing the amplitude of vibrations in operating machinery. Figure 4 shows a schematic view of a cylindrical bearing. The journal spins with angular speed (Ω) and its center (O_j), due to dynamic loads, also describes translational motions within the bearing clearance. The bearing or housing is stationary in most applications. Notable exceptions are those of floating ring journal bearings and automotive reciprocating engine support rod bearings.



**Figure 4: Schematic View of a Cylindrical Journal Bearing.
Fixed Coordinate Systems (θ, z) and Moving Coordinate System (Θ, z) .**

2.1 Reynolds Equation for Journal Bearings

The smallness of this ratio allows for a Cartesian coordinate $(x=R\Theta, y, z)$ to be located on the bearing surface (see Figure 4). Then, in Classical Lubrication, Reynolds equation describes the generation of hydrodynamic pressure (P) within the bearing. This equation arises from integration of the momentum equations (3) across the film thickness and substitution into the continuity equation [2]:

$$\frac{\partial}{\partial t} \{ \rho h \} + \frac{\Omega}{2} \frac{\partial}{\partial \Theta} \{ \rho h \} = \frac{1}{R^2} \frac{\partial}{\partial \Theta} \left\{ \frac{\rho h^3}{12 \mu} \frac{\partial P}{\partial \Theta} \right\} + \frac{\partial}{\partial z} \left\{ \frac{\rho h^3}{12 \mu} \frac{\partial P}{\partial z} \right\} \quad (4)$$

in the flow domain $\{0 \leq \Theta \leq 2\pi, -1/2 L \leq z \leq 1/2 L\}$, where $h(\Theta, z, t)$ is the film thickness, L is the bearing axial length, $U = \Omega R_J$ is the journal surface speed, and (ρ, μ) denote the lubricant density and viscosity, respectively.

The boundary conditions for the hydrodynamic pressure in a **plain** cylindrical bearing are²:

- a) the pressure is continuous and periodic in the circumferential direction, i.e.

$$P(\Theta, z, t) = P(\Theta + 2\pi, z, t) \quad (5)$$

- b) the pressure equals the discharge or atmospheric value (P_a) on the bearing sides, i.e.

$$P(\Theta, \frac{1}{2}L, t) = P(\Theta, -\frac{1}{2}L, t) = P_a \quad (6)$$

As a constraint, the hydrodynamic pressure needs to be greater than the liquid cavitation pressure everywhere in the flow domain, i.e.

$$P \geq P_{cav} \quad \text{in } 0 \leq \Theta \leq 2\pi, \quad -\frac{1}{2}L \leq z \leq \frac{1}{2}L \quad (7)$$

Here P_{cav} represents the lubricant saturation pressure or the ambient pressure needed for release of dissolved gases. In practice, no distinction is made between these two values since hydrodynamic film pressures could be one to two orders of magnitude larger than the ambient value.

Consider the journal and bearing to be aligned and the journal center to have an eccentricity displacement e ($\leq c$). The film thickness is

$$h = c + e \cos(\theta) \quad (8)$$

This formula is accurate for (c/R) ratios as large as 0.10. The film thickness derived assumes rigid bearing and journal surfaces, uniform axial and azimuthal clearance and no journal misalignment.

2.2 Kinematics of Journal Motion

The journal center O_j is displaced a distance (e) from the bearing center O_B . This distance is known as the **journal eccentricity** and may vary with time depending upon the imposed external load on the bearing. The journal eccentricity cannot exceed the bearing clearance, otherwise solid contact and potential catastrophic failure may occur. The eccentricity components in the (X, Y) fixed coordinate system are:

$$e_x = e \cos(\phi); \quad e_y = e \sin(\phi) \quad (9)$$

where ϕ is known as the bearing attitude angle, and $\Theta = \theta + \phi$. Then, the film thickness also equals

$$h = c + e_x \cos \Theta + e_y \sin \Theta = e \sin \theta \quad (10)$$

and

$$\frac{\partial h}{\partial \Theta} = -e_x \sin \Theta + e_y \cos \Theta; \quad \frac{\partial h}{\partial t} = \dot{e}_x \cos \Theta + \dot{e}_y \sin \Theta \quad (11)$$

where $(\dot{})$ denotes differentiation with respect to time, i.e. $(\partial / \partial t)$.

Substitution of the film thickness gradients into Reynolds equation (4) gives the following lubrication equation for an incompressible and isoviscous fluid:

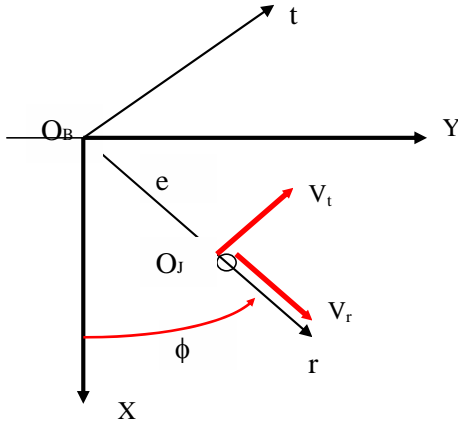
² The simple journal bearing model does not account for feeding holes or axial grooves for supply of the lubricant into the bearing. A more detailed discussion on lubricant cavitation and its physical model can be found in [3].

$$\frac{1}{R^2} \frac{\partial}{\partial \Theta} \left\{ \frac{h^3}{12\mu} \frac{\partial P}{\partial \Theta} \right\} + \frac{\partial}{\partial z} \left\{ \frac{h^3}{12\mu} \frac{\partial P}{\partial z} \right\} = \left\{ \dot{e}_x + e_y \frac{\Omega}{2} \right\} \cos \Theta + \left\{ \dot{e}_y - \frac{\Omega}{2} e_x \right\} \sin \Theta \quad (12)$$

An alternative form of Reynolds equation arises when using the angular coordinate (θ). This angle starts from the location of maximum film thickness. A coordinate system with radial and tangential (r, t) axes is conveniently defined with the unit radial vector along the line joining the bearing and journal centers.

Recall that $e_x = e \cos(\phi)$; $e_y = e \sin(\phi)$, and $e^2 = e_x^2 + e_y^2$.

The journal center velocities in the (X, Y) and (r, t) coordinate systems are related by the transformation:



$$\begin{bmatrix} \dot{e}_x \\ \dot{e}_y \end{bmatrix} = \begin{bmatrix} \cos \phi & -\sin \phi \\ \sin \phi & \cos \phi \end{bmatrix} \begin{bmatrix} \dot{e} \\ e \dot{\phi} \end{bmatrix} \quad (13)$$

Note that $V_r = \dot{e}$, $V_t = e \dot{\phi}$ are the radial and tangential components of the journal translational velocity. From the film thickness $h = c + e \cos \theta$, it follows

Translational velocities of journal center

$$\frac{\partial h}{\partial \theta} = -e \sin \theta \quad (14)$$

$$\frac{\partial h}{\partial t} = \dot{e} \cos \theta - e \frac{\partial \theta}{\partial t} \sin \theta = \dot{e} \cos \theta + e \dot{\phi} \sin \theta = V_r \cos \theta + V_t \sin \theta$$

Thus, Reynolds equation (4) for an incompressible and isoviscous fluid is also expressed as

$$\frac{1}{R^2} \frac{\partial}{\partial \theta} \left\{ \frac{h^3}{12\mu} \frac{\partial P}{\partial \theta} \right\} + \frac{\partial}{\partial z} \left\{ \frac{h^3}{12\mu} \frac{\partial P}{\partial z} \right\} = \dot{e} \cos \theta + e \left\{ \dot{\phi} - \frac{\Omega}{2} \right\} \sin \theta \quad (15)$$

Equation (15) is of particular importance since it allows us to realize an important physical phenomenon. Consider the journal center to describe circular centered orbits with a fixed amplitude or radius, e . Hence $de/dt=0$. Furthermore, if the frequency of whirl equals to 50% of the rotational speed; $\dot{\phi} = \Omega/2$; then the right hand side of Eqn. (15) is null; and hence the pressure is zero, $P=0$ within the bearing film land. There is no generation of hydrodynamic pressure, thus resulting in a sudden loss of load support capability. The 50% sped whirl phenomenon is the basis of rotordynamic instability, as explained later.

2.3 Bearing Reaction Forces

Once the pressure field is obtained, fluid film forces acting on the journal surface, see Figure 5, are calculated by integration of the pressure field acting on the journal surface. An equal opposing force acts on the bearing as well. The bearing reaction forces are expressed in the fixed (X, Y) coordinate system and moving (r, t) coordinate system as

$$\begin{bmatrix} F_X \\ F_Y \end{bmatrix} = \int_0^L \int_0^{2\pi} P(\Theta, z, t) \begin{bmatrix} \cos \Theta \\ \sin \Theta \end{bmatrix} R \cdot d\Theta dz \quad ; \quad \begin{bmatrix} F_r \\ F_t \end{bmatrix} = \int_0^L \int_0^{2\pi} P(\theta, z, t) \begin{bmatrix} \cos \theta \\ \sin \theta \end{bmatrix} R \cdot d\theta dz \quad (16)$$

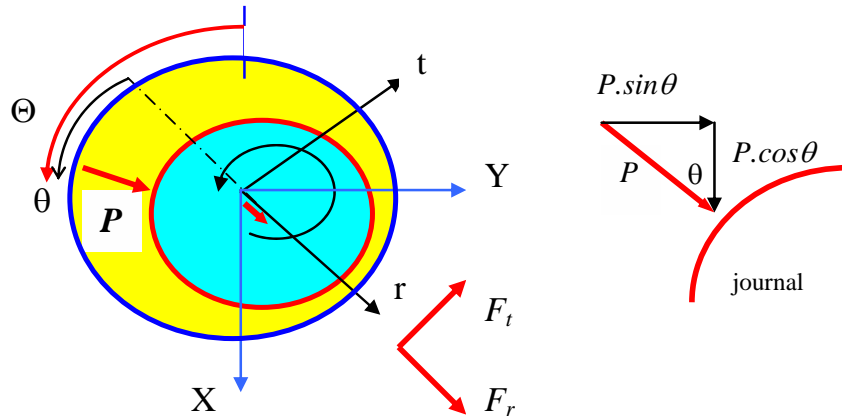


Figure 5: Fluid Film Force Acting on Journal Surface.

The relationship between the fluid film forces in both coordinate systems is given by:

$$\begin{bmatrix} F_X \\ F_Y \end{bmatrix} = \begin{bmatrix} \cos \phi & -\sin \phi \\ \sin \phi & \cos \phi \end{bmatrix} \begin{bmatrix} F_r \\ F_t \end{bmatrix} \quad (16.b)$$

The fluid film forces are generic functions of the journal rotational speed (Ω) and the journal center translational velocities, *i.e.*

$$F_\alpha = F_\alpha(\Omega, \dot{e}_X, \dot{e}_Y) = F_\alpha\left(\dot{e}, e \left[\dot{\phi} - \frac{\Omega}{2} \right]\right); \quad \alpha = X, Y \text{ or } r, t \quad (17)$$

An analytical solution of Reynolds equation for arbitrary geometry cylindrical bearings is not feasible. Most frequently, numerical methods are employed to solve Reynolds equation and to obtain the performance characteristics of bearing configurations of particular interest.

There are analytical solutions to Reynolds equation applicable to two limiting geometries of journal bearings. These are known as the *infinitely long* and *infinitely short* length journal bearing models [2].

In the **LONG BEARING MODEL**, see Figure 6, the length of the bearing is very large, $L/D \rightarrow \infty$, and consequently the axial flow is effectively very small, *i.e.* $(\partial P / \partial z) = 0$.

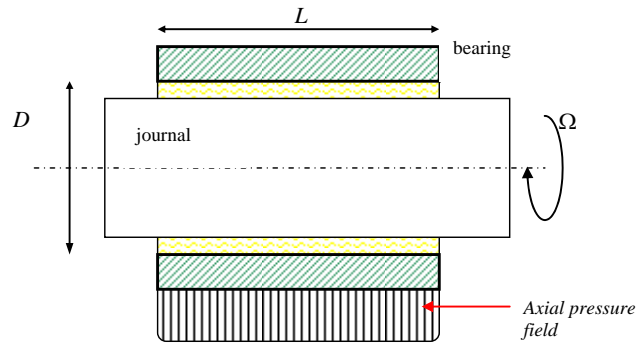


Figure 6: The Long Bearing Model.

For large L/D ratios, Reynolds equation reduces to:

$$\frac{1}{R^2} \frac{\partial}{\partial \theta} \left\{ \frac{h^3}{12\mu} \frac{\partial P}{\partial \theta} \right\} = \frac{\partial}{\partial t} \{h\} + \frac{\Omega}{2} \frac{\partial}{\partial \Theta} \{h\} \quad (18)$$

This bearing model gives accurate results for journal bearings with slenderness ratios $(L/D) > 2$. Most modern bearings in high performance turbomachinery applications have a small L/D ratio, rarely exceeding one. Thus, the infinitely long journal bearing model is of limited current interest. Refer to [2] for details on the analytical solution of Eqn. (18).

This is not the case for squeeze film dampers (SFDs), however, since the long bearing model provides a very good approximation for tightly sealed dampers even for small L/D ratios [4].

3.0 STATIC LOAD PERFORMANCE OF SHORT LENGTH BEARINGS

In this most useful bearing model, see Figure 7, the bearing length is short, $L/D \rightarrow 0$, and consequently the circumferential flow is effectively small, i.e. $(\partial P / \partial \theta) \cong 0$. For this limiting bearing configuration, Reynolds equation reduces to

$$\frac{\partial}{\partial t} \{h\} + \frac{\Omega}{2} \frac{\partial}{\partial \Theta} \{h\} = \frac{\partial}{\partial z} \left\{ \frac{h^3}{12\mu} \frac{\partial P}{\partial z} \right\} \quad (19)$$

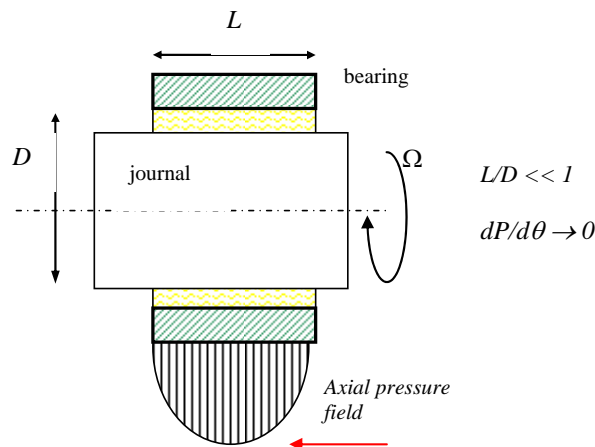


Figure 7: Short Length Bearing Model.

The *short length* bearing model provides (surprisingly) accurate results for plain cylindrical bearings of slenderness ratios $L/D \leq 0.50$ and for small to moderate values of the journal eccentricity, $e \leq 0.75 c$ [4]. The *short length* bearing model is widely used for quick estimations of journal bearing static and dynamic force performance characteristics. Integration of equation (19) leads to the pressure distribution

$$P(\theta, z, t) - P_a = \frac{6\mu \left[\dot{e} \cos \theta + e \left(\dot{\phi} - \frac{\Omega}{2} \right) \sin \theta \right]}{C^3 H^3} \left\{ z^2 - \left(\frac{L}{2} \right)^2 \right\} \quad (20)$$

with $H = h/c = 1 + \varepsilon \cos(\theta)$ as the dimensionless film thickness, and $\varepsilon = e/c$ is the journal eccentricity ratio; [$0 \leq \varepsilon \leq 1$], $\varepsilon = 0$ means centered operation (typically a condition of no load support), and $\varepsilon = 1.0$ evidences solid contact of the journal with its bearing.

No lubricant cavitation will occur if the exit or discharge pressure P_a is well above the liquid cavitation pressure. However, if P_a is low, typically ambient conditions at 1 bar, it is almost certain that the bearing will cavitate or show air entrainment when the outlet plenum is not flooded with lubricant. The *cavitation model* in the short length bearing simply neglects any predicted negative pressures and equates them to zero. This ‘‘chop’’ procedure although theoretically not well justified grasps with some accuracy the actual physics [5]. Hence, if $P_a = 0$, and from equation (21), the pressure field $P > 0$, when $\cos(\theta + \alpha) < 0$. Thus, $P > 0$ in the circumferential region limited by

$$\frac{\pi}{2} \leq \theta + \alpha \leq \frac{3\pi}{2} \rightarrow \frac{\pi}{2} - \alpha = \theta_1 \leq \theta \leq \theta_2 = \frac{3\pi}{2} - \alpha \quad (21)$$

That is, regardless of the type of journal motion, the region of positive pressure has an extent of π ($=180^\circ$); thus then the infamous *π film cavitation model* widely used in the literature.

Fluid film reaction forces on the journal are evaluated by integration of the pressure field acting on the journal surface. With $P_a = 0$, the radial and tangential forces (F_r, F_t) are given by

$$\begin{bmatrix} F_r \\ F_t \end{bmatrix} = -\frac{\mu R L^3}{c^3} \begin{bmatrix} J_3^{02} & J_3^{11} \\ J_3^{11} & J_3^{20} \end{bmatrix} \left(e \left\{ \dot{\phi} - \frac{\Omega}{2} \right\} \right) \quad (22)$$

where the J 's are integrals defined in analytical form by Booker [6]. Note that the fluid film forces are proportional to the journal center translational velocities ($\dot{e}, e\dot{\phi}$) as well as the journal rotational speed (Ω). The reaction forces depend linearly on the fluid viscosity and the bearing radius and grow rapidly with the ratio $(L/C)^3$.

Hydrodynamic journal bearings are designed (and implemented) to support a static load W , hereafter aligned with the X axis for convenience, see Figure 8. At the equilibrium condition, denoted by a journal center eccentric displacement (e) with an attitude angle (ϕ), the hydrodynamic bearing generates a reaction force balancing the applied external load at the rated rotational speed (Ω). The equations of *static equilibrium* are

$$\begin{aligned} W + F_x = 0 &\Rightarrow -W = F_x = F_r \cos \phi - F_t \sin \phi \\ F_y = 0 &\Rightarrow 0 = F_y = F_r \sin \phi + F_t \cos \phi \end{aligned} \quad (23)$$

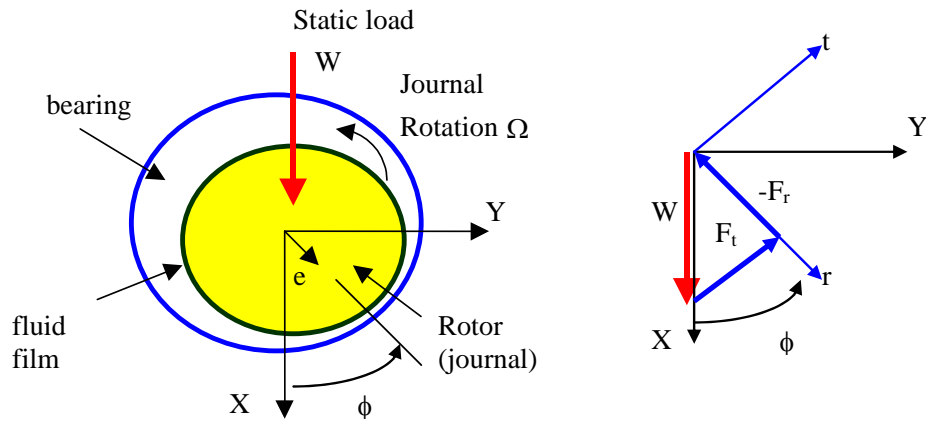


Figure 8: Force Equilibrium for Statically Applied Load.

For static equilibrium, $\dot{e}=0$, $\dot{\phi}=0$, and $\theta_1 = 0$ to $\theta_2 = \pi$. From equation (22), the static radial and tangential film reaction forces are

$$F_r = -\frac{\mu R L^3 \Omega}{c^3} \frac{\varepsilon^2}{(1-\varepsilon^2)^2}; \quad F_t = +\frac{\mu R L^3 \Omega}{c^2} \frac{\pi \cdot \varepsilon}{4(1-\varepsilon^2)^{3/2}} \quad (24)$$

Figure 9 depicts the radial and tangential forces for a typical short length bearing. The forces are proportional to the lubricant viscosity and rotor surface speed (ΩR), the length (L^3), and inversely proportional to the radial clearance (c^2). Most importantly, the bearing forces grow rapidly (non-linearly) with the journal eccentricity ($\varepsilon=e/c$).

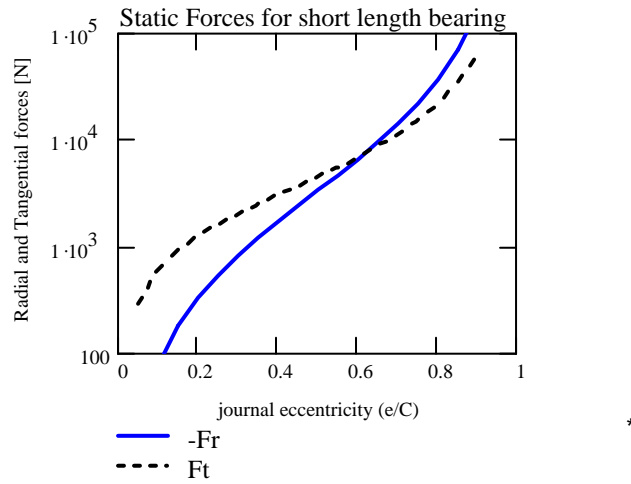


Figure 9: Radial and Tangential Forces for Short Length Bearing.
 $\mu=0.019$ Pa.s, $L=0.05$ m, $c=0.1$ mm, 3,000 rpm, $L/D=0.25$.

The external load (W) is balanced by the fluid film reaction forces. Thus,

$$W = (F_r^2 + F_t^2)^{1/2} = \mu \Omega R L \left(\frac{L}{c}\right)^2 \frac{\varepsilon}{4} \frac{\sqrt{16\varepsilon^2 + \pi^2(1-\varepsilon^2)}}{(1-\varepsilon^2)^2} \quad (25)$$

and the journal attitude angle ϕ is obtained from

$$\text{tang } \phi = -\frac{F_t}{F_r} = \frac{\pi\sqrt{(1-\varepsilon^2)}}{4\varepsilon} \quad (26)$$

Note that as the journal eccentricity $\varepsilon \rightarrow 0$, $\phi \rightarrow \pi/2$, while as $\varepsilon \rightarrow 1$, $\phi \rightarrow 0$.

3.1 Design of Hydrodynamic Bearing – Selection of Operating Eccentricity

In the design of hydrodynamic journal bearings, the bearing static performance characteristics are related to a unique dimensionless parameter known as the **Sommerfeld Number (S)** defined as

$$S = \frac{\mu N L D}{W} \left(\frac{R}{c}\right)^2 \quad (27)$$

where $N = (\Omega/2\pi)$ is the rotational speed in revolutions/sec. In practice, the specific load or pressure is known as the ratio of applied load to bearing projected area, i.e. (W/LD).

In short length journal bearings, a modified Sommerfeld number (σ) is defined and related to (S) by [5, 7]:

$$\sigma = \pi S (L/D)^2 = \frac{\mu \Omega L R}{4W} \left(\frac{L}{C}\right)^2 \quad (28)$$

Substitution of Eqn. (28) into Eqn. (25) relates the modified Sommerfeld number to the equilibrium operating journal eccentricity (e), i.e.

$$\frac{\mu \Omega L R}{4W} \left(\frac{L}{c}\right)^2 = \sigma = \frac{(1-\varepsilon^2)^2}{\varepsilon\sqrt{\{16\varepsilon^2 + \pi^2(1-\varepsilon^2)\}}} \quad (29)$$

At a rated operating condition, σ is known since the bearing geometry (R, L, c), rotational speed (Ω), fluid viscosity (μ) and applied load (W) are known. Then, equation (29) provides a relationship to determine (iteratively) the equilibrium journal eccentricity ratio $\varepsilon = (e/c)$ required to generate the fluid film reaction force balancing the externally applied load W .

Figures 10 and 11 depict the modified Sommerfeld number and attitude angle vs. journal eccentricity, respectively. Large Sommerfeld (σ) numbers; i.e. denoting small load, high speed Ω or large lubricant viscosity, determine small operating journal eccentricities or nearly centered operation, $\varepsilon \rightarrow 0$, $\phi \rightarrow \pi/2$ (90°). That is, the journal eccentricity vector is nearly orthogonal to the applied load.

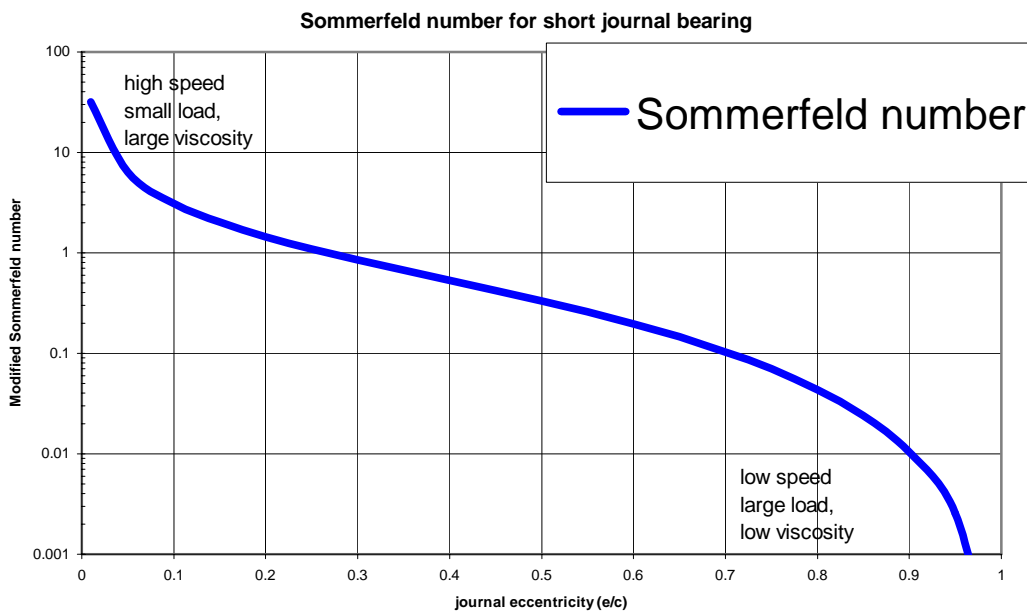


Figure 10: Modified Sommerfeld (σ) Number versus Journal Eccentricity.

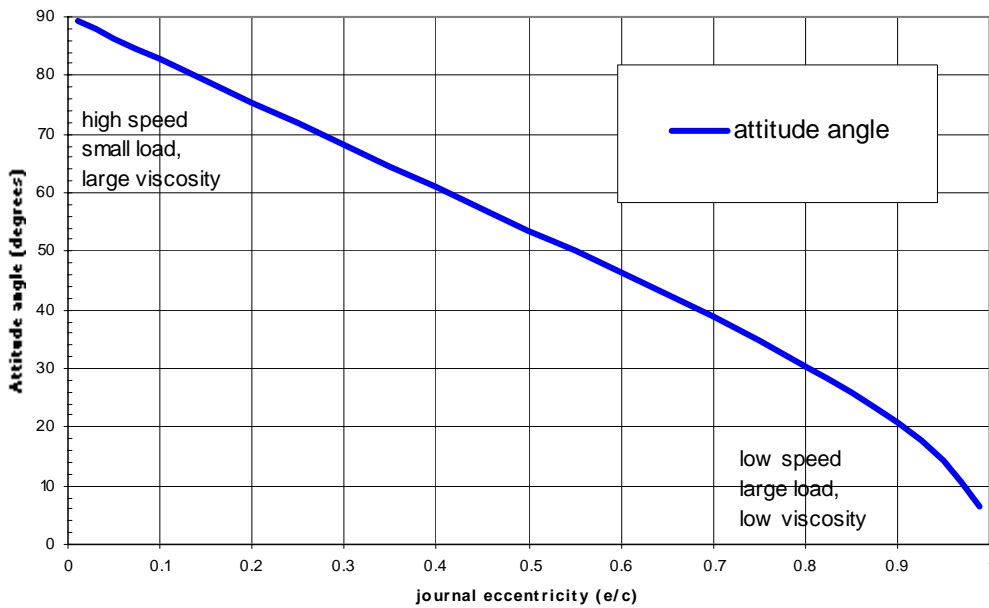


Figure 11: Equilibrium Attitude Angle versus Journal Eccentricity.

Small Sommerfeld (σ) numbers, i.e. denoting large load, low speed Ω or low lubricant viscosity, determine large operating journal eccentricities, $\varepsilon \rightarrow 1.0$, $\phi \rightarrow 0$ (0°). Note that the journal eccentricity vector is nearly parallel to the applied load.

Figure 12 shows the journal displacement within the bearing clearance for different operating conditions. The journal eccentricity approaches the clearance for large loads, low shaft speeds or light lubricant viscosity, and it is aligned with the load vector. For small loads, high speeds or large lubricant viscosities

(large Sommerfeld numbers), the journal travels towards the bearing center and its position is **orthogonal** to the applied load. This peculiar behavior is the source of rotordynamic instability as will be shown shortly.

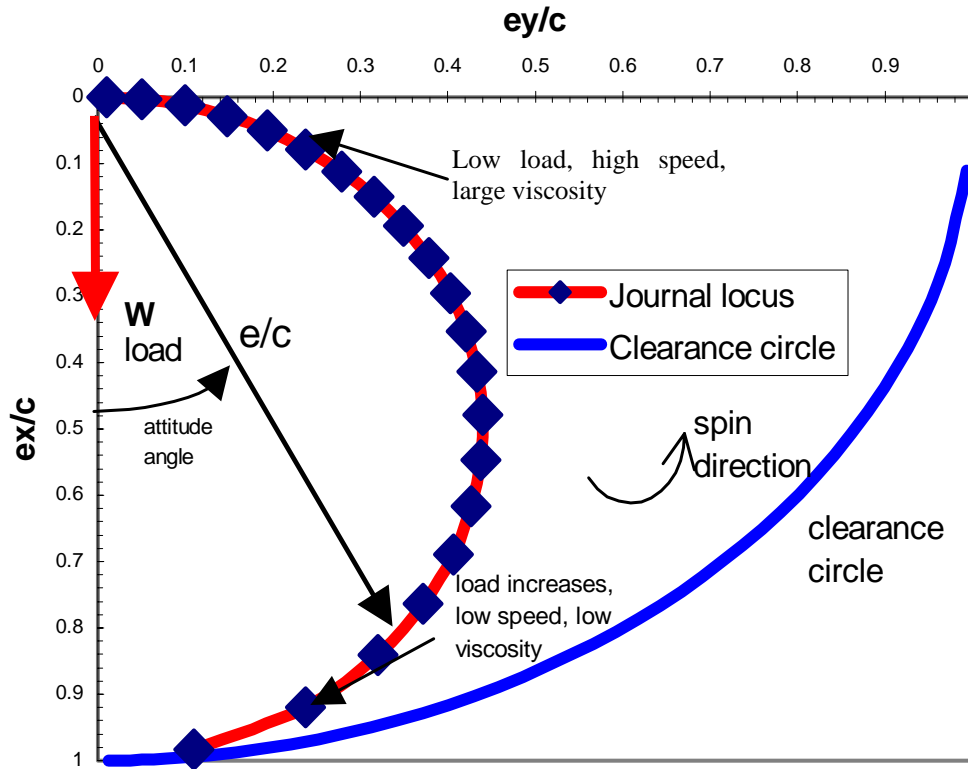


Figure 12: Locus of Journal Center for Short Length Bearing.

4.0 DYNAMICS OF A RIGID ROTOR SUPPORTED ON SHORT LENGTH BEARINGS

Figure 13 depicts a symmetric rigid rotor of mass $2M$, and supporting a static load ($2F_o=W$) along the X axis. The rotor is mounted on two identical plain hydrodynamic journal bearings. The equations of motion of the rotating system at constant rotational speed (Ω) are given by [5]:

$$\begin{aligned} M \ddot{X} &= F_x + M u \Omega^2 \sin(\Omega t) + F_o \\ M \ddot{Y} &= F_y + M u \Omega^2 \cos(\Omega t) \end{aligned} \quad (30)$$

where u is the magnitude of the imbalance vector, $X(t)$ and $Y(t)$ are the coordinates of the rotor mass center, and (F_x, F_y) are the fluid film bearing reaction forces. Since the rotor is rigid, the center of mass displacements are identical to those of the journal bearings, i.e. $X(t) = e_x(t)$, $Y(t) = e_y(t)$

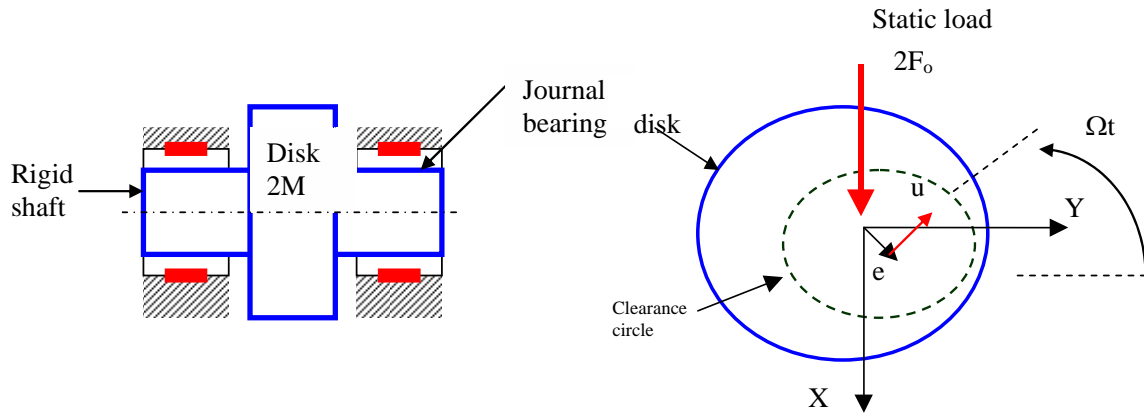
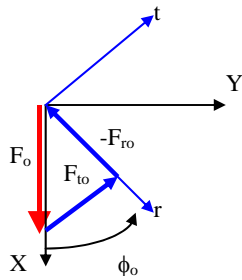


Figure 13: Rigid Rotor Supported on Journal Bearings.
(u) Imbalance, (e) Journal Eccentricity.

We are interested on the rotor dynamic behaviour for small amplitude motions about the equilibrium position defined by:

$$F_{X_o} = -F_o, \quad F_{Y_o} = 0, \quad \Rightarrow e_{X_o}, e_{Y_o} \text{ or } e_o, \phi_o \quad (31)$$

where (e_o, ϕ_o) denote the static equilibrium journal eccentricity and attitude angle, respectively. The bearing static reaction forces satisfy



$$\begin{aligned} F_o + F_{X_o} = 0 &\Rightarrow F_o = F_{X_o} = F_{r_o} \cos \phi_o - F_{t_o} \sin \phi_o \\ F_{Y_o} = 0 &\Rightarrow 0 = F_{Y_o} = F_{r_o} \sin \phi_o + F_{t_o} \cos \phi_o \end{aligned} \quad (32)$$

Small amplitude journal motions about the equilibrium position, as represented in Figure 14, are defined as:

$$e_x = e_{X_o} + \Delta e_x(t), \quad e_y = e_{Y_o} + \Delta e_y(t), \quad \text{or } X = X_o + \Delta X(t), \quad Y = Y_o + \Delta Y(t) \quad (33a)$$

$$\text{or conversely,} \quad e(t) = e_o + \Delta e(t), \quad \phi(t) = \phi_o + \Delta \phi(t) \quad (33b)$$

$$\begin{aligned} \text{with} \quad \frac{dX}{dt} = \dot{e}_x = \Delta \dot{e}_x, \quad \frac{dY}{dt} = \dot{e}_y = \Delta \dot{e}_y \\ \frac{d^2 X}{dt^2} = \ddot{e}_x = \Delta \ddot{e}_x, \quad \frac{d^2 Y}{dt^2} = \ddot{e}_y = \Delta \ddot{e}_y \end{aligned} \quad (33c)$$

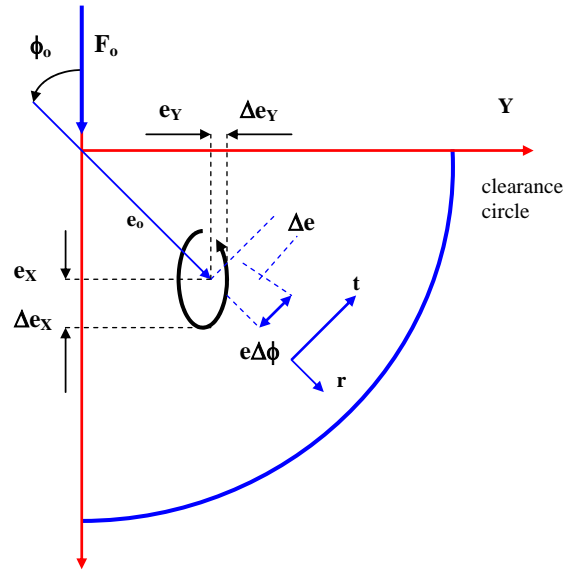


Figure 14: Small Amplitude Journal Motions about an Equilibrium Position.

The journal dynamic displacements in the (r, t) coordinate system are related to those in the (X, Y) system by the linear transformation

$$\begin{bmatrix} \Delta e_x \\ \Delta e_y \end{bmatrix} = \begin{bmatrix} \cos \phi_o & -\sin \phi_o \\ \sin \phi_o & \cos \phi_o \end{bmatrix} \begin{bmatrix} \Delta e(t) \\ e_o \Delta \phi(t) \end{bmatrix} \quad (34)$$

Similar relationships hold for the journal center velocities and accelerations. Note that the assumption of small amplitude motions requires $\Delta e_x, \Delta e_y \ll c$, i.e., the journal dynamic displacements are smaller than the bearing clearance.

Recall that the fluid film forces are general functions of the journal center displacements and velocities, i.e. $F_\alpha = F_\alpha [e_x(t), e_y(t), \dot{e}_x(t), \dot{e}_y(t)]$, $\alpha = X, Y$. Now, express the bearing reaction forces as a Taylor Series expansion around the static journal position (e_{Xo}, e_{Yo}) , i.e.

$$\begin{aligned} F_X &= F_{Xo} + \frac{\partial F_X}{\partial X} \Delta X + \frac{\partial F_X}{\partial Y} \Delta Y + \frac{\partial F_X}{\partial \dot{X}} \Delta \dot{X} + \frac{\partial F_X}{\partial \dot{Y}} \Delta \dot{Y} \\ F_Y &= F_{Yo} + \frac{\partial F_Y}{\partial X} \Delta X + \frac{\partial F_Y}{\partial Y} \Delta Y + \frac{\partial F_Y}{\partial \dot{X}} \Delta \dot{X} + \frac{\partial F_Y}{\partial \dot{Y}} \Delta \dot{Y} \end{aligned} \quad (35)$$

4.1 Definition of Dynamic Force Coefficients in Fluid Film Bearings

Fluid film bearing stiffness $(K_{ij})_{ij=X,Y}$ and damping $(C_{ij})_{ij=X,Y}$ force coefficients are defined as

$$K_{ij} = -\frac{\partial F_i}{\partial X_j} \quad ; \quad C_{ij} = -\frac{\partial F_i}{\partial \dot{X}_j} \quad i, j=X, Y \quad (36)$$

For example, $K_{XY} = -\partial F_X / \partial Y$ corresponds to a stiffness produced by a fluid force in the X direction due to a journal static displacement in the Y direction. By definition, this coefficient is evaluated at the equilibrium

position with other journal center displacements and velocities set to *zero*. The negative sign in the definition ensures that a positive magnitude stiffness coefficient corresponds to a restorative force.

The force coefficients (K_{XX} , K_{YY}) are known as the **direct** stiffness terms, while (K_{XY} , K_{YX}) are referred as *cross-coupled*. Figure 15 provides a pictorial representation of the bearing force coefficients as mechanical parameters.

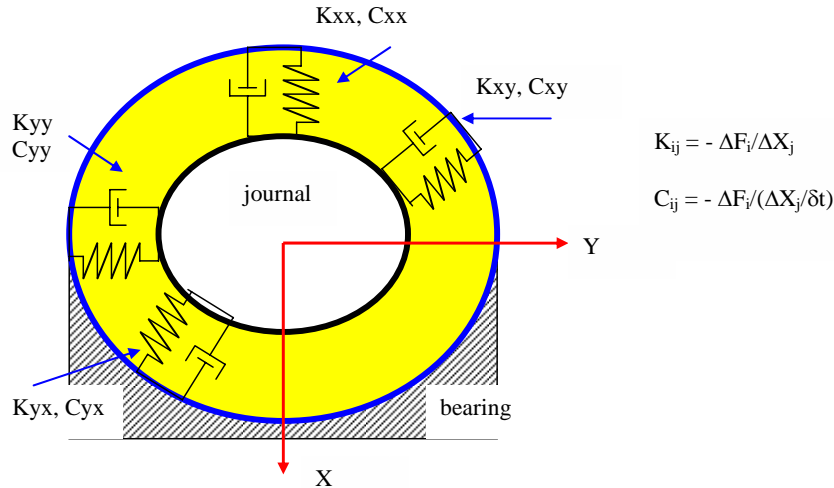


Figure 15: The “Physical Representation” of Stiffness and Damping Coefficients in Lubricated Bearings.

Inertia or added mass coefficients $\{M_{ij}\}_{i,j=X,Y}$ can also be defined as $M_{ij} = -\frac{\partial F_i}{\partial \ddot{X}_j}$; $i,j=X,Y$ where $\{\ddot{X}, \ddot{Y}\}$ are

journal center accelerations. Inertia coefficients are of particular importance in super laminar and turbulent flow fluid film bearings and annular seals. The inertia force coefficients or *apparent* masses have a sound physical interpretation. These coefficients are always present in a fluid film bearing. Inertia coefficients can be of large magnitude, in particular for dense liquids. However, the effect of inertia forces on the dynamic response of rotor-bearing systems is only of importance at large excitation frequencies, i.e. high squeeze film Reynolds numbers. (This fact also holds for most mechanical systems subjected to fast transient motions).

With the given definitions, the bearing reaction forces are represented as

$$\begin{pmatrix} F_X(t) \\ F_Y(t) \end{pmatrix} = \begin{pmatrix} F_{Xo} \\ F_{Yo} \end{pmatrix} - \begin{bmatrix} K_{XX} & K_{XY} \\ K_{YX} & K_{YY} \end{bmatrix} \begin{pmatrix} \Delta X \\ \Delta Y \end{pmatrix} - \begin{bmatrix} C_{XX} & C_{XY} \\ C_{YX} & C_{YY} \end{bmatrix} \begin{pmatrix} \Delta \dot{X} \\ \Delta \dot{Y} \end{pmatrix} \quad (37)$$

where $F_{Xo} = F_o = 1/2W$ and $F_{Yo} = 0$. Note that the defined force coefficients allow the representation of the dynamic fluid film bearing (or seal) forces in terms of the fundamental mechanical parameters $\{K, C, \text{ and } M\}$. However, this does not mean that these force coefficients must be accordance with accepted “physics grounded” knowledge. For example, the “viscous” damping coefficients may be negative, i.e. non-dissipative, or the stiffness coefficients non-restorative.

From Eqn. (30), the linear equations for small amplitude motions of the rotor-bearing system are

$$\begin{bmatrix} M & O \\ O & M \end{bmatrix} \begin{pmatrix} \Delta \ddot{X} \\ \Delta \ddot{Y} \end{pmatrix} + \begin{bmatrix} C_{XX} & C_{XY} \\ C_{YX} & C_{YY} \end{bmatrix} \begin{pmatrix} \Delta \dot{X} \\ \Delta \dot{Y} \end{pmatrix} + \begin{bmatrix} K_{XX} & K_{XY} \\ K_{YX} & K_{YY} \end{bmatrix} \begin{pmatrix} \Delta X \\ \Delta Y \end{pmatrix} = M u \Omega^2 \begin{pmatrix} \cos \Omega t \\ \sin \Omega t \end{pmatrix} \quad (38)$$

The literature presents the force coefficients in dimensionless form according to the definition:

$$k_{ij} = K_{ij} \frac{c}{F_0}; \quad c_{ij} = C_{ij} \frac{c\Omega}{F_0} \quad i,j=X,Y \quad (39)$$

where F_o is the static load applied on each bearing (along the X direction). [Note that the total static load $W=2F_o$ is shared by the two bearings in a symmetric rotor mount].

Lund [8] derived first the analytical formulas for the short bearing force coefficients. Figures 16 and 17 depict the dimensionless force coefficients, stiffness and damping, as functions of the journal eccentricity and of the modified Sommerfeld number (σ), respectively. In the figures, both representations are necessary since at times the journal eccentricity is known a priori; while most often, the design parameter, i.e. the Sommerfeld number, is known in advance. In general, the physical magnitude of the stiffness and damping coefficients increases rapidly (nonlinearly) as the journal eccentricity increases.

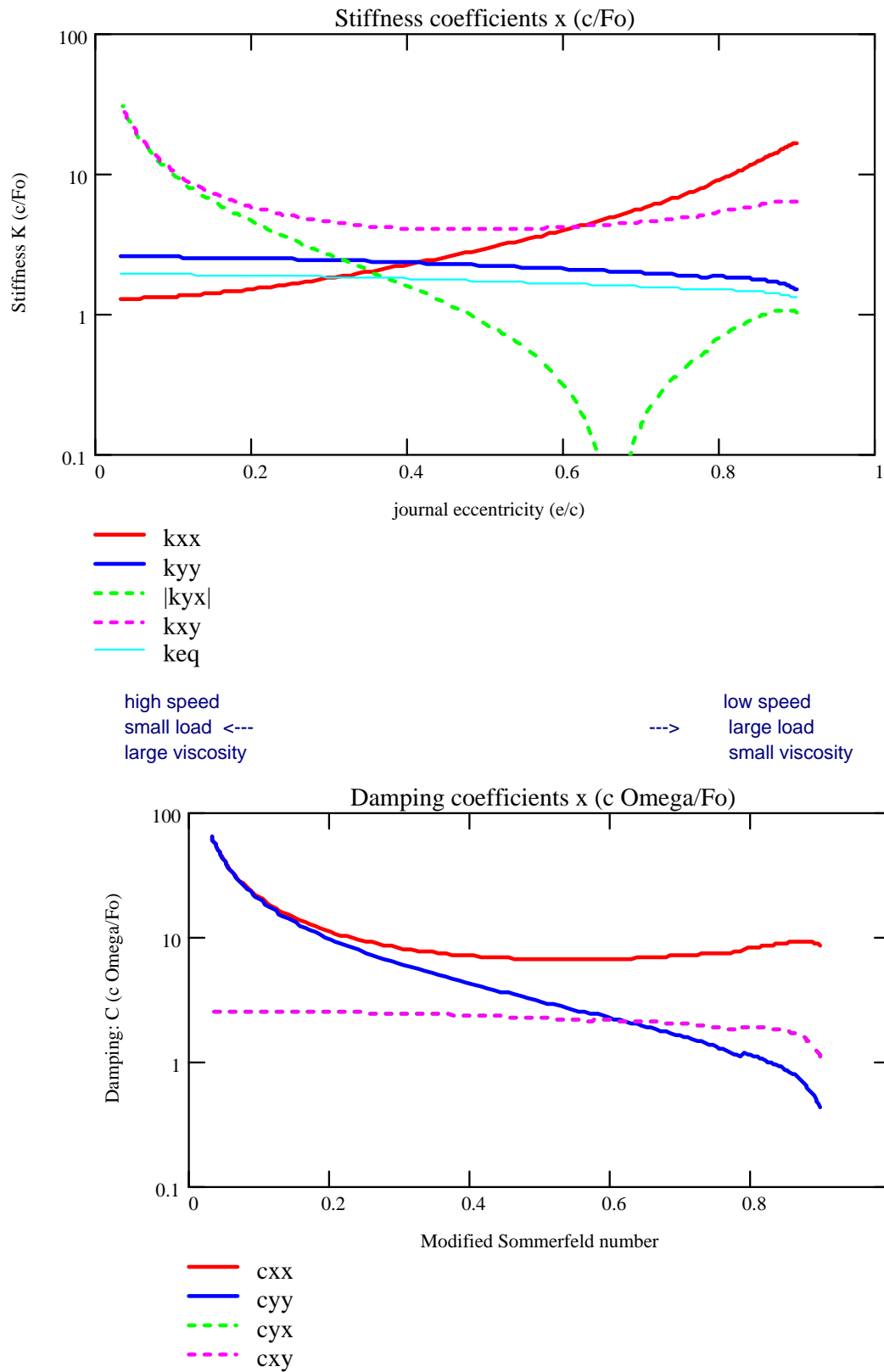


Figure 16: Dimensionless Stiffness and Damping Coefficients vs. Journal Eccentricity (ϵ) for Short Journal Bearing.

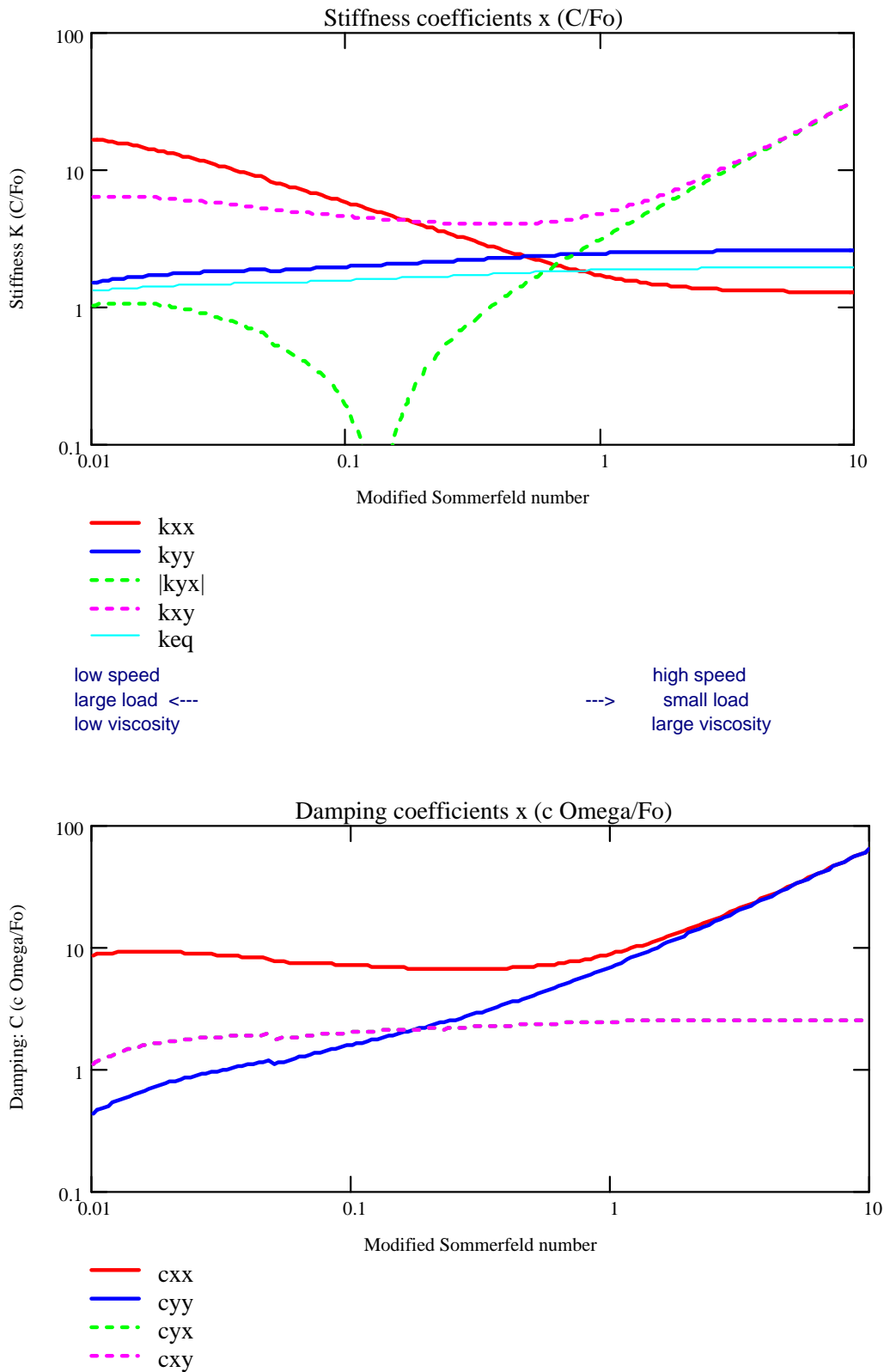


Figure 17: Dimensionless Stiffness and Damping Coefficients vs. Sommerfeld Number (σ) for Short Journal Bearing.

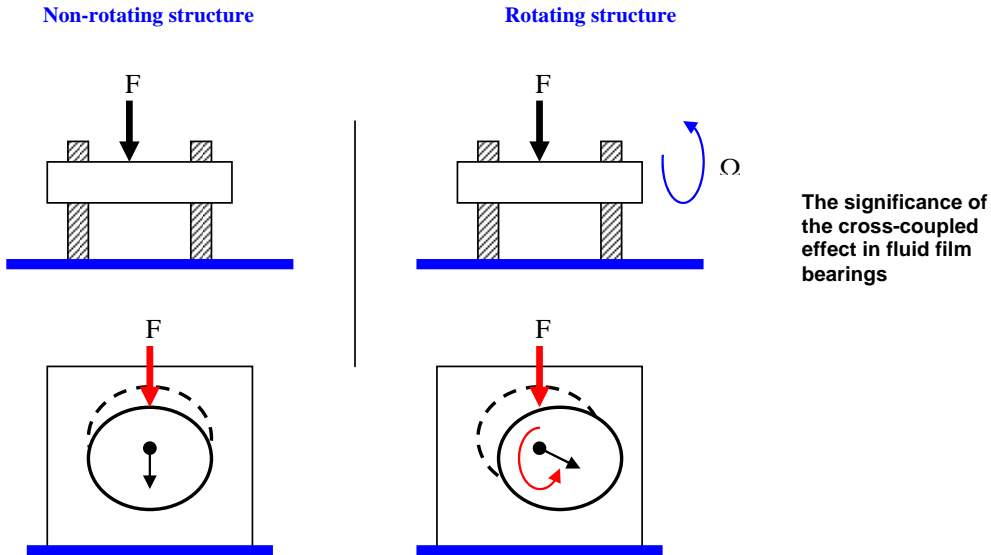
Note that the dimensionless force coefficients do not represent the actual physical trends. For example, at $e_o=0$, $K_{XX}=K_{YY}=0$, but the dimensionless $k_{XX}=k_{YY}$ have non zero value. This peculiarity follows from the definition of dimensionless force coefficients using the applied load (F_o). Recall that, as $e_o \rightarrow 0$, the static load F_o is also naught.

4.2 Dynamic Force Coefficients for Journal Centered Operation, i.e. No Applied Load

As the journal center approaches the bearing center, $e_o \rightarrow 0$, $\phi_o = 90^\circ$, and from the formulas presented,

$$K_{XY} = -K_{YX} = \bar{k} = \frac{\mu \Omega R L^3 \pi}{c^3} \frac{\pi}{4} = \frac{\Omega}{2} \bar{c}; \quad C_{XX} = C_{YY} = \bar{c} = \frac{\mu R L^3 \pi}{c^3} \frac{\pi}{2} \quad (40)$$

Thus, at the centered journal position a hydrodynamic bearing offers no direct (support) stiffness but only cross-coupled forces. A small load applied on the bearing will cause a journal displacement in a direction orthogonal (transverse) to the load, as shown in the schematic view below. This behaviour is common to all fluid film journal bearings of rigid geometry.



5.0 ROTORDYNAMIC STABILITY OF RIGID ROTOR SUPPORTED ON SHORT LENGTH BEARINGS

The linearized equations of motion are written in dimensionless form as [5, 9]

$$p^2 \begin{bmatrix} \Delta x'' \\ \Delta y'' \end{bmatrix} + \begin{bmatrix} c_{XX} & c_{XY} \\ c_{YX} & c_{YY} \end{bmatrix} \begin{bmatrix} \Delta x' \\ \Delta y' \end{bmatrix} + \begin{bmatrix} k_{XX} & k_{XY} \\ k_{YX} & k_{YY} \end{bmatrix} \begin{bmatrix} \Delta x \\ \Delta y \end{bmatrix} = p^2 \delta \begin{bmatrix} \cos(\tau) \\ \sin(\tau) \end{bmatrix} \quad (41)$$

where $\Delta x = \frac{\Delta X}{c}$, $\Delta y = \frac{\Delta Y}{c}$, $\tau = \Omega t$, $\delta = \frac{u}{c}$, $(\cdot) = \frac{d}{d\tau}$; $p^2 = \frac{C M \Omega^2}{F_o}$ is a dimensionless mass, and k_{ij} and c_{ij} are the dimensionless stiffness and damping force coefficients.

It is of interest to determine if the rotor-bearing system is **stable** for small amplitude journal center motions (perturbations) about the equilibrium position. To this end, set the imbalance parameter $\delta = 0$ in the equations above to obtain,

$$p^2 \begin{bmatrix} \Delta x'' \\ \Delta y'' \end{bmatrix} + \begin{bmatrix} c_{XX} & c_{XY} \\ c_{YX} & c_{YY} \end{bmatrix} \begin{bmatrix} \Delta x' \\ \Delta y' \end{bmatrix} + \begin{bmatrix} k_{XX} & k_{XY} \\ k_{YX} & k_{YY} \end{bmatrix} \begin{bmatrix} \Delta x \\ \Delta y \end{bmatrix} = \begin{bmatrix} 0 \\ 0 \end{bmatrix} \quad (42)$$

If the rotor-bearing system is to become **unstable**, this will occur at a **threshold speed of rotation** (Ω_s) and the rotor will perform (undamped)³ orbital motions at a whirl frequency (ω_s). These motions, satisfying equation (42), are of the form:

$$x = A e^{j\omega_s t} = A e^{j\bar{\omega} \tau}; \quad y = B e^{j\omega_s t} = B e^{j\bar{\omega} \tau}; \quad j = \sqrt{-1} \quad (43)$$

where $\bar{\omega} = \omega_s / \Omega_s$ is known as the **whirl frequency ratio**, i.e. the ratio of the rotor whirl or precessional frequency to the rotor onset speed of instability. Substitution of (43) into equation (42) leads to [5]:

$$\begin{bmatrix} -p_s^2 \bar{\omega}_s^2 + k_{XX} + j\bar{\omega}_s c_{XX} & k_{XY} + j\bar{\omega}_s c_{XY} \\ k_{YX} + j\bar{\omega}_s c_{YX} & -p_s^2 \bar{\omega}_s^2 + k_{YY} + j\bar{\omega}_s c_{YY} \end{bmatrix} \begin{bmatrix} A \\ B \end{bmatrix} = \begin{bmatrix} 0 \\ 0 \end{bmatrix} \quad (44)$$

In Eqn. (44), the determinant Δ , must be zero for a non-trivial solution of the homogenous system. After algebraic manipulation, the real and imaginary parts of Δ render [5,9]

$$p_s^2 \bar{\omega}_s^2 = k_{eq} = \frac{k_{XX} c_{YY} + k_{YY} c_{XX} - c_{YX} k_{XY} - c_{XY} k_{YX}}{c_{XX} + c_{YY}} = \frac{CM\omega_s^2}{F_o} \quad (45)$$

and

$$\bar{\omega}_s^2 = \frac{(k_{eq} - k_{XX})(k_{eq} - k_{YY}) - k_{XY} \cdot k_{YX}}{c_{XX} c_{YY} - c_{XY} c_{YX}} = \left(\frac{\omega_s}{\Omega_s} \right)^2 \quad (46)$$

5.1 Threshold Speed, Critical Mass, Equivalent Stiffness and Whirl Frequency Ratio

For a given value of journal eccentricity (ε_o), i.e. a given Sommerfeld number (σ), one evaluates Eqn. (45) to obtain the equivalent stiffness k_{eq} , and then Eqn. (46) to get the whirl frequency ratio $\bar{\omega}_s$. This substitution then yields $p_s^2 = k_{eq} / \bar{\omega}_s^2$ (~critical mass), which in turn renders the onset speed of instability Ω_s .

Figures 18 and 19 depict the whirl frequency ratio (ω/Ω)_s and the **dimensionless** threshold speed of instability (p_s) versus equilibrium journal eccentricity and modified Sommerfeld number, respectively. Note that for near centered journal operation, i.e. large Sommerfeld numbers, the whirl frequency is 0.50, i.e. half-synchronous whirl.

³ Recall that in a mechanical system, an equivalent damping ratio > 0 causes the attenuation of motions induced by small perturbations from an equilibrium position. A null damping ratio brings the system into sustained periodic motions without decay or growth, thus denoting the threshold between stability and instability (amplitude growing motions).

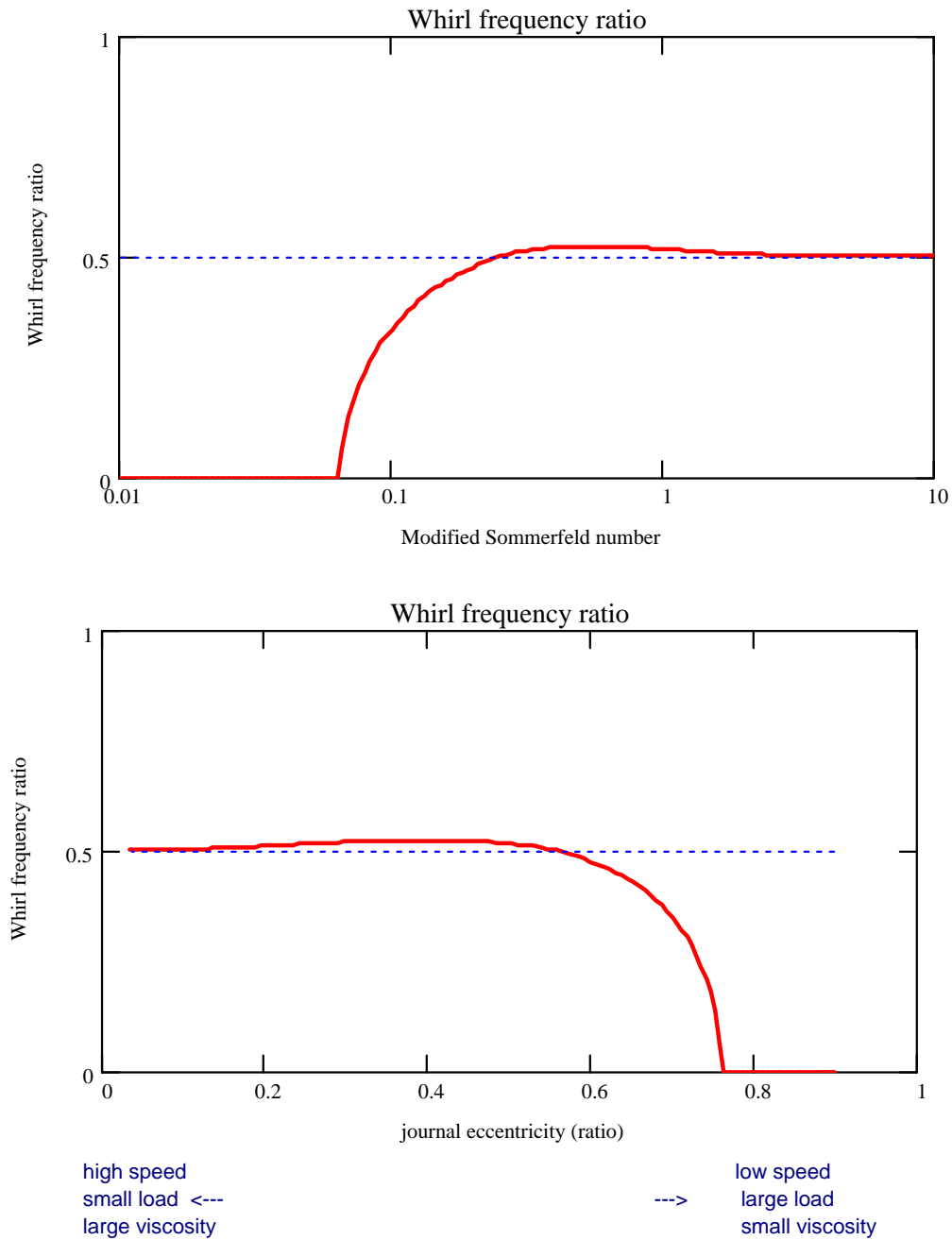


Figure 18: Whirl Frequency Ratio vs. Sommerfeld Number (σ) and Journal Eccentricity (ϵ).

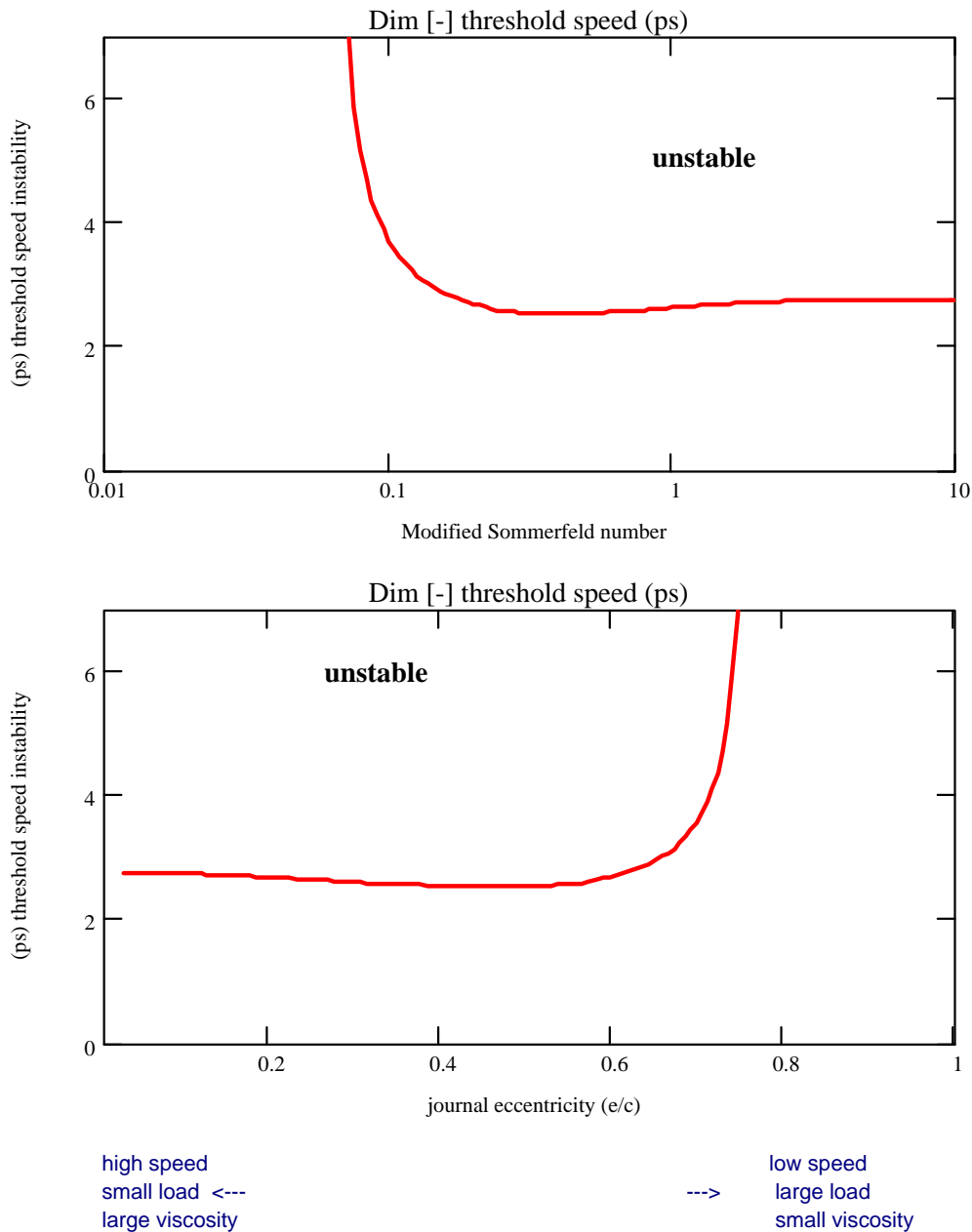


Figure 19: Threshold Speed of Instability (p_s) vs. Sommerfeld Number (σ) and Journal Eccentricity (ϵ).

On the other hand, if one assumes that the current rotational speed (Ω) is the onset speed of instability, then from the relations above it follows the largest magnitude of $\frac{1}{2}$ system mass (M) to make the rotor-bearing system unstable. This mass is known as the **critical mass**, M_c , and corresponds to the limit mass which the system can carry dynamically. If the rotor mass is equal to or larger than twice M_c , then the system will become unstable at the rated speed Ω ⁴.

The whirl frequency ratio (WFR), ω_s/Ω_s , is the ratio of the rotor whirl frequency to the *onset speed of instability*. Note that this ratio, as given in equation (46), depends only on the fluid film bearing

⁴ Recall that each bearing carries half the static load, and also half the dynamic or inertia load ($2.M_c C \Omega^2$).

characteristics and the equilibrium eccentricity. The *WFR* is independent of the rotor characteristics (rotor mass and flexibility) [5]. Reference [10] presents an analysis including fluid inertia effects, more applicable to annular pressure seals and bearings handling process fluids of large density.

The parameter k_{eq} is a journal bearing (dimensionless) equivalent stiffness, also depicted in Figures 16 and 17. From the definitions of threshold speed and whirl ratio, $p_s^2 = M \Omega_s^2 (C/F_o)$ and $\bar{\omega}_s = \omega_s / \Omega_s$, then

$$M \omega_s^2 = k_{eq} \left(\frac{F_o}{C} \right) = K_{eq} \quad (47)$$

Thus, the whirl or precessional frequency is

$$\omega_s = \sqrt{\frac{K_{eq}}{M}} = \omega_n \quad (48)$$

i.e., the whirl frequency equals the **natural frequency** of the rigid rotor supported on journal bearings.

For operation close to the concentric position, $\varepsilon_o \rightarrow 0$, i.e. large Sommerfeld numbers (no load condition), the force coefficients are, see equation (40),

$$k_{XX} = k_{YY} = 0; \quad c_{XX} = c_{YY}; \quad k_{XY} = -k_{YX}; \quad c_{XY} = c_{YX} = 0 \quad (49)$$

$$k_{eq} = (k_{XX} c_{XX} + c_{XY} k_{XY}) / c_{XX} = 0$$

and

$$\frac{\omega_s}{\Omega_s} = \frac{k_{XY}}{c_{XX}} = 0.50 \quad \text{as } \varepsilon \rightarrow 0 \quad (50)$$

This value of whirl frequency ratio (*WFR*) is a characteristic of hydrodynamic plain journal bearings. The *WFR* shows that at the onset speed of instability the rotor whirls at its natural frequency equal to 50% of the threshold rotational speed. Furthermore, under no externally applied loads, $F_o=0$, as in vertically turbomachinery, the bearing possesses no support stiffness, i.e. $K_{eq}=0$ and the system natural frequency (ω_n) is zero, i.e. the rotor-bearing system must whirl at all operating speeds.

Note that if $K_{XY} = 0$, i.e. the bearing does not have cross-coupled effects, then the *WFR* = 0, i.e. no whirl occurs and the system is always dynamically stable. Cross-coupled effects are then responsible for the instabilities so commonly observed in rotors mounted on journal bearings. If the whirl frequency ratio is 0.50, then the maximum rotational speed that the rotor-bearing system can attain is just,

$$\Omega_{\max} = \frac{\omega_s}{0.50} = 2\omega_s = 2\omega_n \quad (51)$$

i.e., twice the natural frequency (or observed rigid rotor critical speed).

Figures 18, 19 and 20 depict the whirl frequency ratio, the dimensionless threshold speed (p_s) and the critical mass (p_s)² versus the Sommerfeld number and equilibrium journal eccentricity. The results demonstrate that a rigid-rotor supported on plain journal bearings is **STABLE** for journal eccentricity ratios $\varepsilon > 0.75$ (small *Sommerfeld numbers*) for all *L/D* ratios. Note that the critical mass and whirl frequency ratio are nearly invariant for operation with journal eccentricities (ε_o) below 0.50.

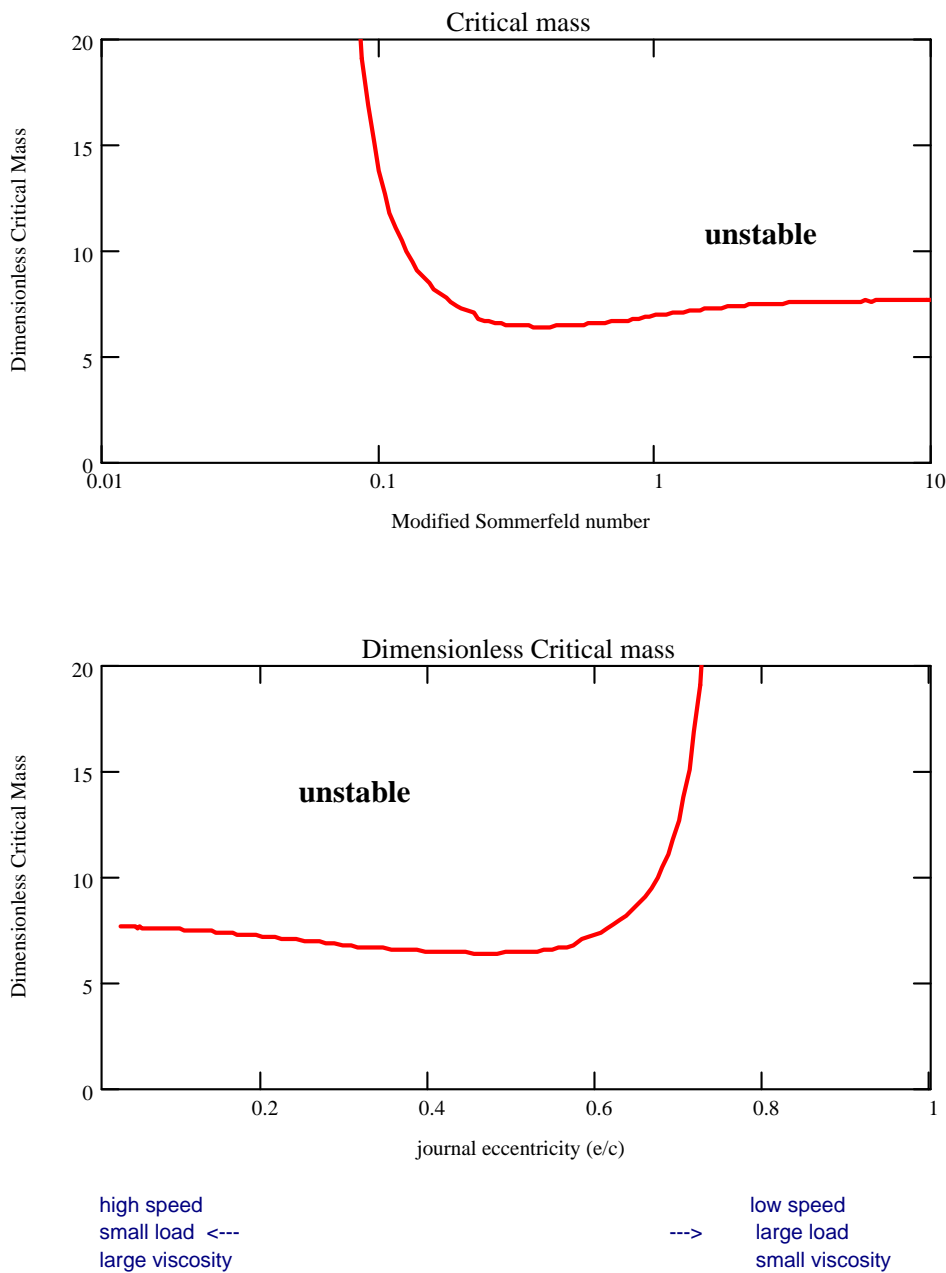
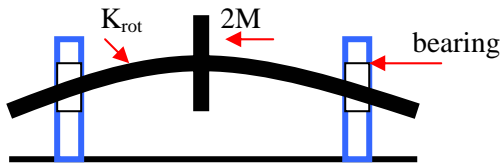


Figure 20: Critical Mass ($m_c = p_s^2$) vs. Sommerfeld Number (σ) and Journal Eccentricity (ϵ).

Keep in mind that increasing the rotational speed of the rotor-bearing system determines larger Sommerfeld numbers, and consequently, operation at smaller journal eccentricities for the same applied static load. Thus, operation at ever increasing speeds will eventually lead to a rotor dynamically unstable system as the analysis results show.

5.2 Effects of Rotor Flexibility on Stability of System

A similar analysis can be performed considering rotor flexibility [5, 11]. This analysis is more laborious though straightforward. The analysis shows that rotor flexibility does not affect the whirl frequency ratio. However, the onset speed of instability is dramatically reduced since the natural frequency of the rotor-bearing system is much lower. The relationship for the threshold speed of instability of a flexible rotor is:



$$p_{sf}^2 = \frac{P_s^2}{1 + k_{eq} \left(\frac{T}{C} \right)} \quad (52)$$

where the sub index f denotes a flexible rotor. K_{rot} is the rotor stiffness on each side of the mid disk shown in the graph, and $T = F_o / K_{rot}$ is the rotor static **sag** or elastic deformation at midspan.

The elastic shaft and bearing are mounted in series, i.e. the bearing and shaft flexibilities add (reciprocal of stiffnesses), and thus the equivalent system stiffness is lower than that of the bearings, and therefore the system natural frequency decreases significantly.

Figure 21 depicts the threshold speed of instability (p_{sf}) for a flexible rotor mounted on plain short length journal bearings. Note that the more flexible the rotor is, the lower the threshold speed of instability. If the fluid film bearings are designed too stiff (low Sommerfeld numbers), then the natural frequency of the rotor-bearing system is just $(K_{rot}/M)^{1/2}$, irrespective of the bearing configuration.

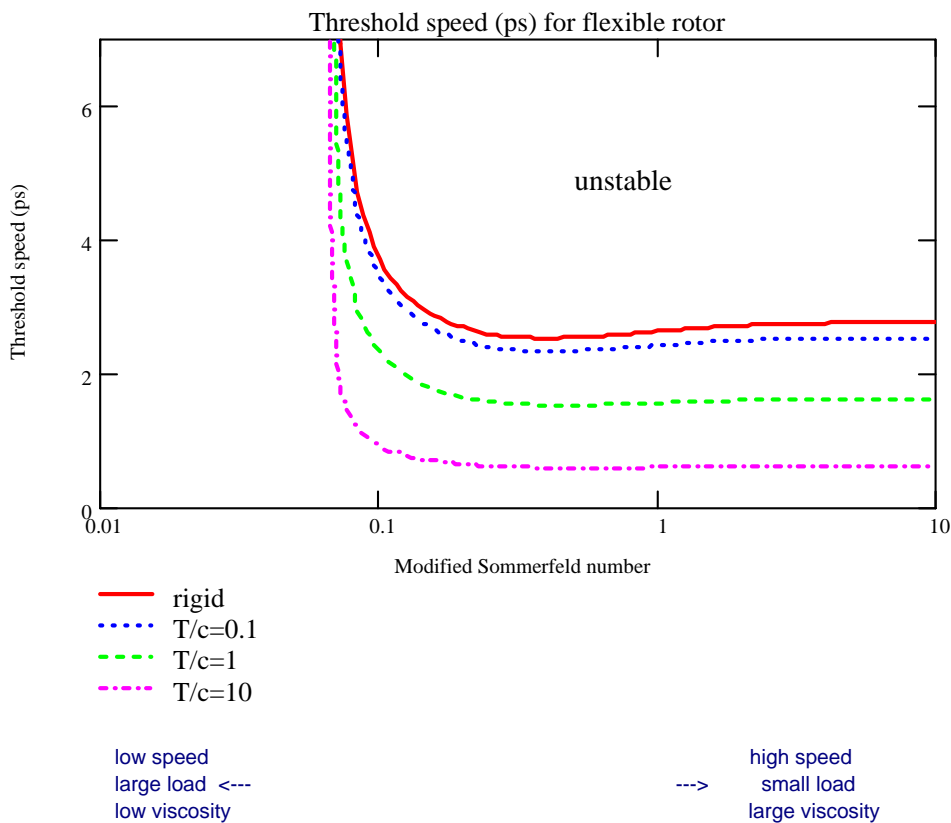


Figure 21: Threshold Speed of Instability (p_s) for Flexible Rotor versus Sommerfeld Number (σ). Static Sag (T/c) Varies.

5.3 Physical Interpretation of Dynamic Forces for Circular Centered Whirl

The bearing dynamic forces in the radial and tangential are

$$\begin{pmatrix} F_r \\ F_t \end{pmatrix}_d = - \begin{bmatrix} K_{rr} & K_{rt} \\ K_{tr} & K_{tt} \end{bmatrix} \begin{pmatrix} \Delta e \\ e_0 \Delta \phi \end{pmatrix} - \begin{bmatrix} C_{rr} & C_{tr} \\ C_{tr} & C_{tt} \end{bmatrix} \begin{pmatrix} \Delta \dot{e} \\ e_0 \Delta \dot{\phi} \end{pmatrix} \quad (53)$$

Consider circular journal motions of amplitude Δe at a forward frequency (ω), as shown in Figure 22. At the centered position, the bearing has no direct stiffnesses, only cross-coupled stiffness and direct damping, i.e.

$$K_{rr} = K_{tt} = C_{rt} = C_{tr} = 0 \quad (54)$$

$$\bar{K} = K_{rt} = -K_{tr} = \frac{\Omega}{2} \bar{C}; \quad \bar{C} = C_{tt} = C_{rr} = \frac{\mu RL^3}{C^3} \frac{\pi}{2}$$

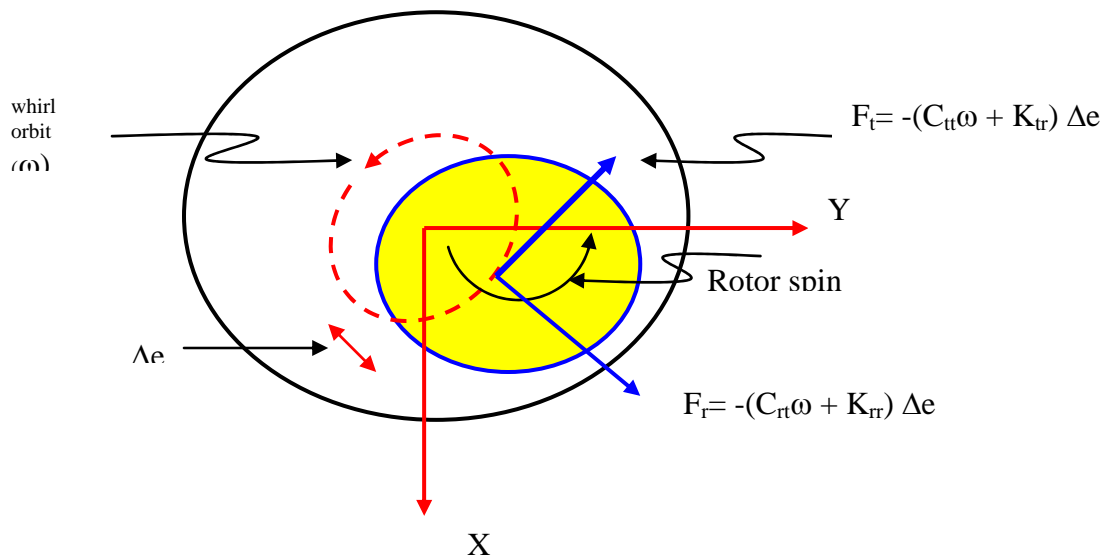


Figure 22: Force Diagram for Circular Centered Whirl Motions.

And thus, the radial and tangential forces become

$$F_{r_d} = 0; \quad F_{t_d} = -(C_{tr} \omega - K_{rt}) \Delta e \quad (55)$$

A destabilizing force will drive the journal in the direction of the forward whirl motion, i.e. $F_t > 0$ if the equivalent damping (C_{eq}) is negative (see Figure 23), i.e.

$$\left(C_{tr} - \frac{1}{\omega} K_{rt} \right) = C_{eq} < 0 \quad (56)$$

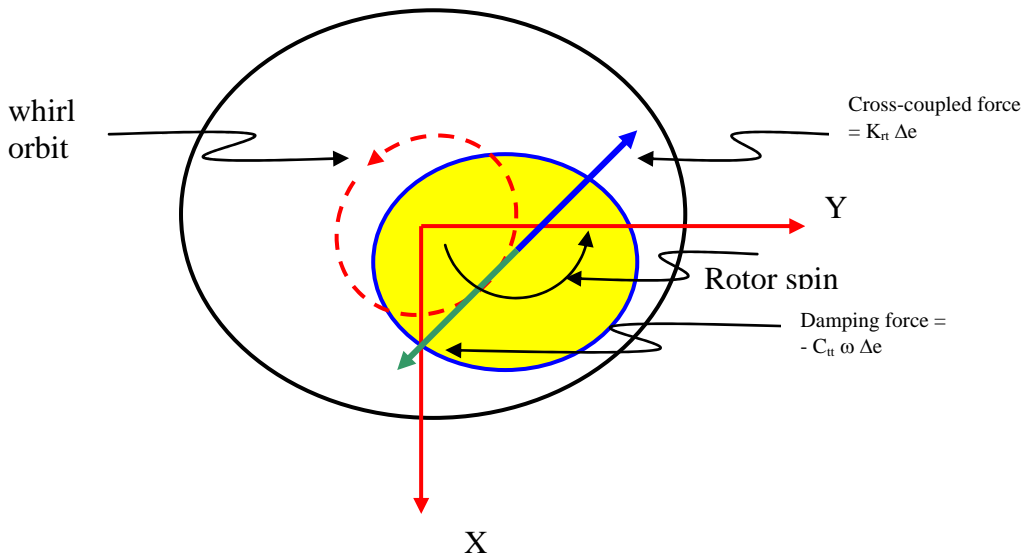


Figure 23: Forces Driving and Retarding Rotor Whirl Motion.

At the threshold speed of instability, $K_{rt} = \frac{\Omega}{2} C_{rt}$. Thus, unstable forward whirl motions occur for rotor speeds $\Omega \geq 2\omega_s$.

In the (X, Y) coordinate system, $\Delta X = \Delta e \cos(\omega t)$ and $\Delta Y = \Delta e \sin(\omega t)$. Thus, the bearing dynamic forces become

$$\begin{pmatrix} F_X \\ F_Y \end{pmatrix}_d = - \begin{pmatrix} + \sin(\omega t) \\ - \cos(\omega t) \end{pmatrix} \left(\frac{\Omega}{2} - \omega \right) C_{xx} \Delta e = C_{xx} \left(1 - \frac{\Omega}{2\omega} \right) \begin{pmatrix} + \sin(\omega t) \\ - \cos(\omega t) \end{pmatrix} \omega \Delta e = \tag{57}$$

$$\begin{pmatrix} F_X \\ F_Y \end{pmatrix}_d = - C_{xx} \left(1 - \frac{\Omega}{2\omega} \right) \begin{pmatrix} \Delta \dot{X} \\ \Delta \dot{Y} \end{pmatrix}$$

Note that (F_X, F_Y) oppose the forward whirl motion for journal speeds $\Omega < 2\omega_s$. For larger rotor speeds, the bearing forces become positive and aid to the growth of the forward whirl amplitude of motion, as shown graphically in Figure 24.

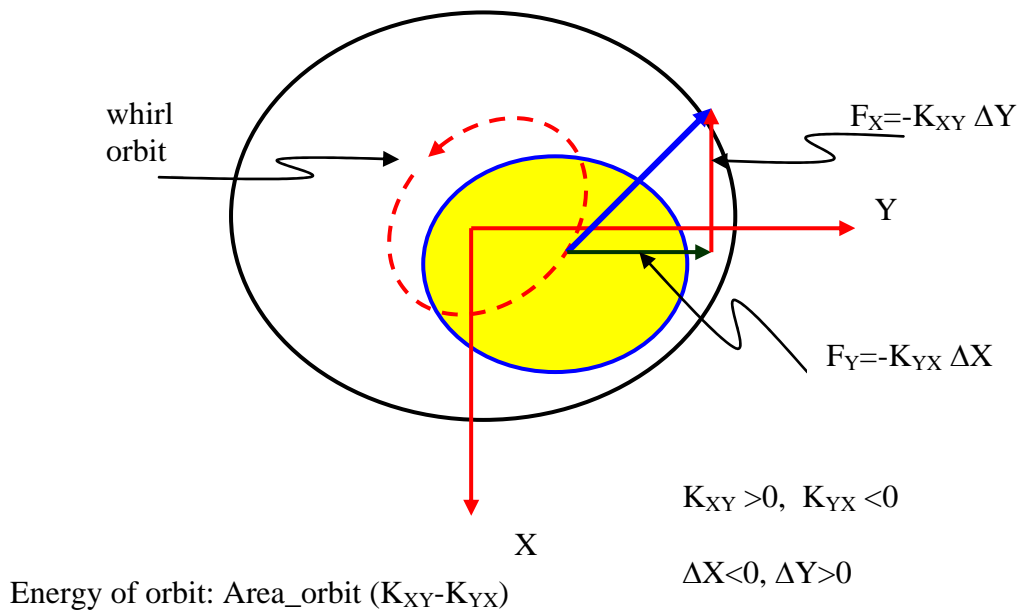


Figure 24: Representation of Follower Force from Cross-Coupled Stiffnesses.

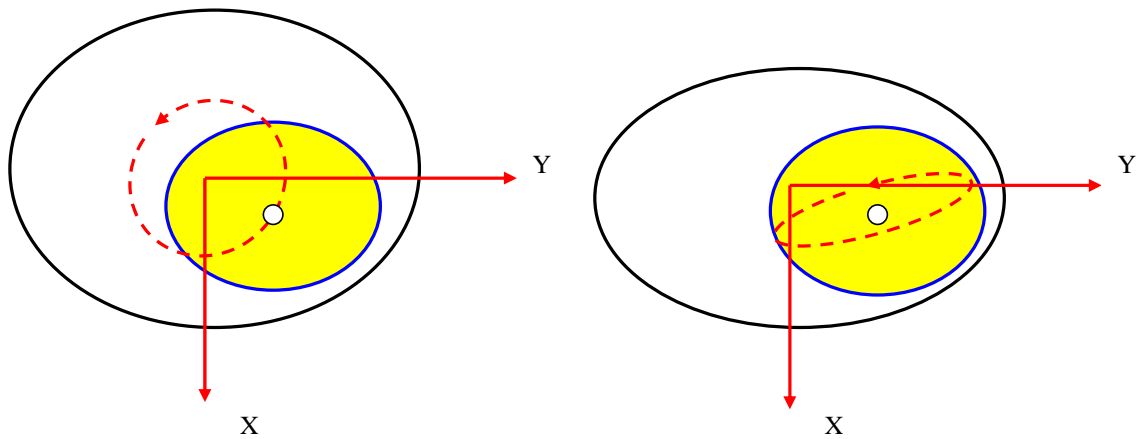
The work performed by the bearing forces during a full orbital period ($T = 2\pi/\omega$) equals [9]

$$E = \oint (F_{X_d} \Delta \dot{X}_{(t)} + F_{Y_d} \Delta \dot{Y}_{(t)}) dt = \oint (F_r \omega \Delta e) dt = -(C_{tt} \omega - K_{rr}) \omega \Delta e^2 T = \quad (58)$$

$$E = -(2\pi \Delta e^2) (C_{tt} \omega - K_{rr}) = -2 Area_{orbit} C_{eq} \omega$$

Note that $E < 0$ is equivalent to negative work, i.e. energy removed or dissipated from the rotor-bearing system. However when $E > 0$, i.e. for $\Omega \geq 2\omega_s$, the fluid film bearing adds "energy" into the rotor-bearing system thus driving the whirl motion forward.

From this discussion one can easily deduce that rotor-bearings evidencing whirl orbits with skewed areas (sharp ellipsoids) will be less prone to rotordynamic instability, see Figure 25. This type of dynamic response is obtained by design and construction of a bearing generating (direct) stiffness asymmetry, as given in multiple pad bearing configurations (elliptic, multiple-lobe with preloads, pressure-dam bearings). However, these bearings are limited to fixed orientation static loads and rotor spin in only one direction.



Energy of orbit: Area $\times (K_{XY} - K_{YX})$

Figure 25: Influence of Bearing Asymmetry on Whirl Orbits.

5.4 Experimental Measurements of Rotor-Bearing System Instability

The archival literature is abundant in experimental and field descriptions of severe instabilities induced by fluid film bearings on rotating machinery. As an example of tests conducted at the author's laboratory on a high speed test rig, Figure 26 depicts recorded amplitudes of motion versus shaft speed in a rigid rotor supported on plain journal bearings. The displacement measurements correspond to rotor motions along the vertical and horizontal planes (LV, LH). The curves with larger amplitudes denote the total amplitudes of motion while the others in light color show the filtered synchronous (1X) motions with slow roll compensation. The passage through a well-damped critical speed is evident at ~ 8.5 krpm. As the shaft speed increases, the amplitudes of motion decrease. However, at a shaft speed \sim twice the critical speed, the rotor becomes violently unstable with large amplitude motions nearly equalling the bearings' clearances.

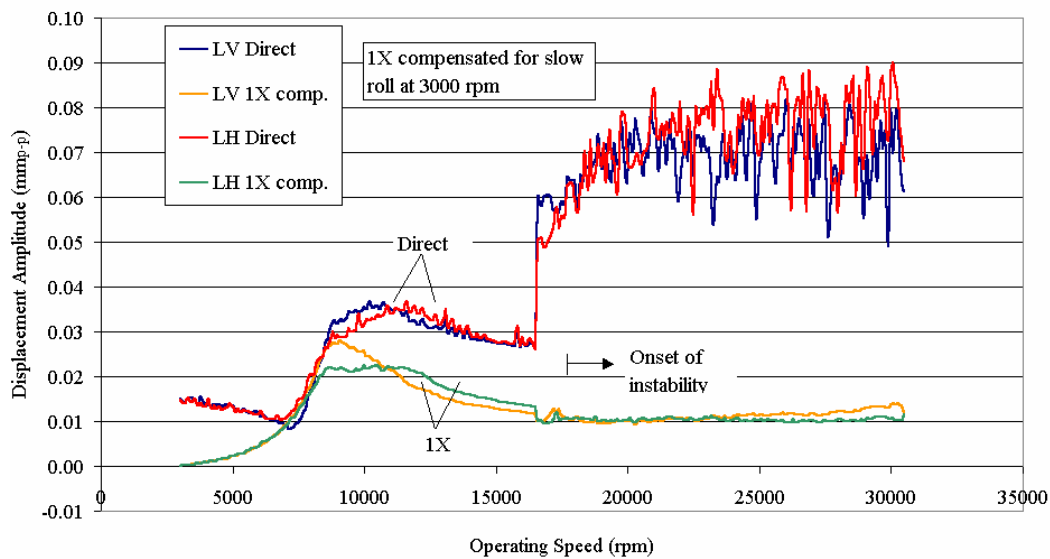


Figure 26: Amplitudes of Rotor Motion versus Shaft Speed. Experimental Evidence of Rotordynamic Instability.

Figure 27 depicts the waterfall of the vertical shaft motion. The graph shows the frequency content of the vibration signal as the rotor accelerates. The synchronous motions are denoted by the 1X line. The whirl frequency ratio is 0.50 at the onset of the severe subsynchronous motions. As the speed increases, the whirl frequency locks at the system natural frequency. This phenomenon is known as oil-whip. The rotor was severely damaged upon completion of the experiment.

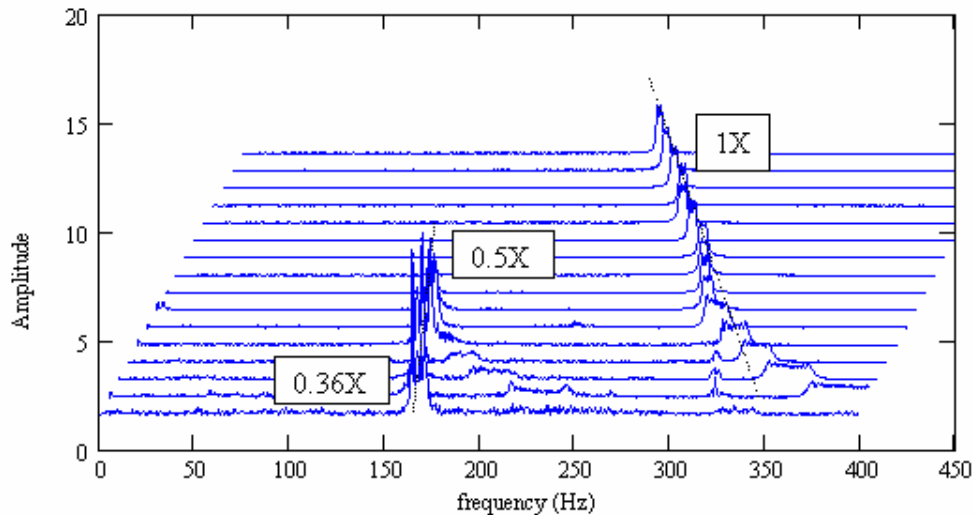


Figure 27: Waterfall of Recorded Rotor Motion Demonstrating Subsynchronous Whirl.

6.0 CLOSURE

Compressors, turbines, pumps, electric motors, electric generators and other rotating machines are commonly supported on fluid film bearings. In the past, most applications implemented common cylindrical plain journal bearings. As machines have achieved higher speeds and larger power, rotor dynamic instability problems such as oil whirl have brought the need to implement other bearing configurations. Cutting axial grooves in the bearing to supply oil flow into the lubricated surfaces generates some of these geometries. Other bearing types have various patterns of variable clearance (preload and offset) to create a pad film thickness that has strongly converging and diverging regions, thus generating a direct stiffness for operation even at the journal centered position. Various other geometries have evolved as well, such as the tilting pad bearing, which allows each pad to pivot, and thus to take its own equilibrium position. This feature usually results in a strongly converging film region for each loaded pad and the near absence of cross-coupled stiffness coefficients.

Tables 2 and 3 summarize some of the advantages and disadvantages of various bearings in condensed form. Figure 28 shows graphical sketches for some of the bearing configurations below. References [12, 13, 14] offer important technical information on the design, operation and stability considerations for the most common fluid film bearings used in industrial applications, with emphasis in pumps and compressors.

Table 2: Fixed Pad Non-Pre Loaded Journal Bearings

Bearing Type	Advantages	Disadvantages	Comments
Plain Journal	<ol style="list-style-type: none"> 1. Easy to make 2. Low Cost 	<ol style="list-style-type: none"> 1. Most prone to oil whirl 	Round bearings are nearly always “crushed” to make elliptical bearings
Partial Arc	<ol style="list-style-type: none"> 1. Easy to make 2. Low Cost 3. Low horsepower loss 	<ol style="list-style-type: none"> 1. Poor vibration resistance 2. Oil supply not easily contained 	Bearing used only on rather old machines
Axial Groove	<ol style="list-style-type: none"> 1. Easy to make 2. Low Cost 	<ol style="list-style-type: none"> 1. Subject to oil whirl 	Round bearings are nearly always “crushed” to make elliptical or multi-lobe
Floating Ring	<ol style="list-style-type: none"> 1. Relatively easy to make 2. Low Cost 	<ol style="list-style-type: none"> 1. Subject to oil whirl (two whirl frequencies from inner and outer films (50% shaft speed, 50% [shaft + ring] speeds) 	Used primarily on high speed turbochargers for PV and CV engines
Elliptical	<ol style="list-style-type: none"> 1. Easy to make 2. Low Cost 3. Good damping at critical speeds 	<ol style="list-style-type: none"> 1. Subject to oil whirl at high speeds 2. Load direction must be known 	Probably most widely used bearing at low or moderate rotor speeds
Offset Half (With Horizontal Split)	<ol style="list-style-type: none"> 1. Excellent suppression of whirl at high speeds 2. Low Cost 3. Easy to make 	<ol style="list-style-type: none"> 1. Fair suppression of whirl at moderate speeds 2. Load direction must be known 	High horizontal stiffness and low vertical stiffness - may become popular - used outside U.S.
Three and Four Lobe	<ol style="list-style-type: none"> 1. Good suppression of whirl 2. Overall good performance 3. Moderate cost 	<ol style="list-style-type: none"> 1. Expensive to make properly 2. Subject to whirl at high speeds 	Currently used by some manufacturers as a standard bearing design

Table 3: Pad Journal Bearings with Steps, Dams or Pockets, Tilting Pad Bearing

Bearing Type	Advantages	Disadvantages	Comments
Pressure Dam (Single Dam)	<ol style="list-style-type: none"> 1. Good suppression of whirl 2. Low cost 3. Good damping at critical speeds 4. Easy to make 	<ol style="list-style-type: none"> 1. Goes unstable with little warning 2. Dam may be subject to wear or build up over time 3. Load direction must be known 	<p>Very popular in the petrochemical industry. Easy to convert elliptical over to pressure dam</p>
Multi-Dam Axial Groove or Multiple-Lobe	<ol style="list-style-type: none"> 1. Dams are relatively easy to place in existing bearings 2. Good suppression of whirl 3. Relatively low cost 4. Good overall performance 	<ol style="list-style-type: none"> 1. Complex bearing requiring detailed analysis 2. May not suppress whirl due to non bearing causes 	<p>Used as standard design by some manufacturers</p>
Hydrostatic	<ol style="list-style-type: none"> 1. Good suppression of oil whirl 2. Wide range of design parameters 3. Moderate cost 	<ol style="list-style-type: none"> 1. Poor damping at critical speeds 2. Requires careful design 3. Requires high pressure lubricant supply 	<p>Generally high stiffness properties used for high precision rotors</p>

NON-FIXED PAD JOURNAL BEARINGS

Bearing Type	Advantages	Disadvantages	Comments
Tilting Pad Journal Bearing	<ol style="list-style-type: none"> 1. Will not cause whirl (no cross coupling) 	<ol style="list-style-type: none"> 1. High Cost 2. Requires careful design 3. Poor damping at critical speeds 	<p>Widely used bearing to stabilize machines with subsynchronous non-bearing related excitations</p>
Flexure Pivot, Tilting Pad Bearing		<ol style="list-style-type: none"> 4. Hard to determine actual clearances 5. Load direction must be known 	
Foil Bearing	<ol style="list-style-type: none"> 1. Tolerance to misalignment. 2. Oil-free 	<ol style="list-style-type: none"> 1. High cost 2. Dynamic performance not well known for heavily loaded machinery 3. Prone to subsynchronous whirl 	<p>Used mainly for low load support on high speed machinery (APU units)</p>

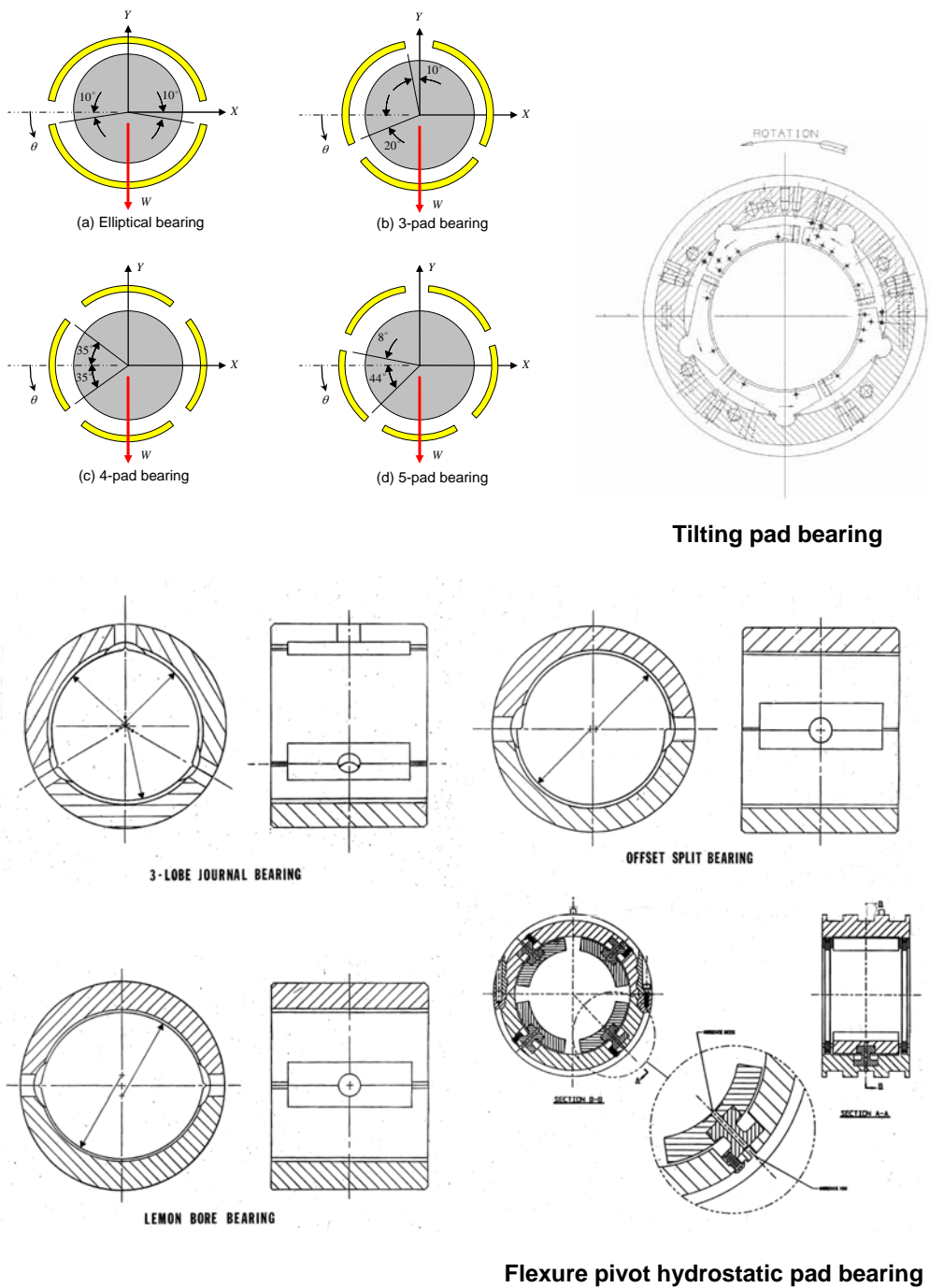


Figure 28: Schematic Views of Various Radial Fluid Film Bearing Configurations.

REFERENCES

- [1] Turbulence in Fluid Film Bearings, L. San Andrés, Lecture Notes (#8) in Modern Lubrication, <http://phn.tamu.edu/TRIBGroup>, 2002.
- [2] Tribology – Friction, Lubrication & Wear, A. Szeri, Hemisphere Pubs, 1980.

- [3] Cavitation in Liquid Film Bearings, L. San Andrés, Lecture Notes (#6) in Modern Lubrication, <http://phn.tamu.edu/TRIBGroup>, 2002.
- [4] Effect of Fluid Inertia on Finite Length Sealed Squeeze Film Dampers, L. San Andrés & J.M. Vance, ASLE Transactions, **30**, 3, pp. 384-393, 1987.
- [5] Turbomachinery Rotordynamics, (chapter 3), D. Childs, John Wiley & Sons, Inc., 1993.
- [6] A Table of the Journal Bearing Integrals, J.F. Booker, ASME Journal of Basic Engineering, pp. 533-535, 1965.
- [7] Rotordynamics of Turbomachinery, J.M. Vance, J., Wiley Inter-Science Pubs., 1988.
- [8] Self-Excited, Stationary Whirl Orbits of a Journal in a Sleeve Bearing, J. Lund, Ph.D. Thesis, Rensselaer Polytechnic Institute, Troy, N.Y., 1966.
- [9] Dynamics of Simple Rotor-Fluid Film Bearing System, L. San Andrés, Lecture Notes (#5) in Modern Lubrication, <http://phn.tamu.edu/TRIBGroup>, 2002.
- [10] Effect of Eccentricity on the Force Response of a Hybrid Bearing, L. San Andrés, STLE Tribology Transactions, **34**, 4, pp. 537- 544, 1991.
- [11] The Stability of an Elastic Rotor in Journal Bearings with Flexible Supports, J. Lund, ASME Journal of Applied Mechanics, pp. 911-920, 1965.
- [12] Design of Journal Bearings for Rotating Machinery, P. Allaire & R.D. Flack, Proc. of the 10th Turbomachinery Symposium, TAMU, pp. 25-45, 1981.
- [13] Fluid Film Bearing Fundamentals and Failure, F. Zeidan & B. Herbage, Proc. of the 20th Turbomachinery Symposium, TAMU, pp. 161-186. 1991.
- [14] Fundamentals of Fluid Film Journal Bearing Operation and Modeling, M. He & J. Byrne, Proc. of the 34th Turbomachinery Symposium, TAMU, pp. 155-176, 2005.